Atmos. Meas. Tech. Discuss., 6, 8679–8741, 2013
www.atmos-meas-tech-discuss.net/6/8679/2013/
doi:10.5194/amtd-6-8679-2013

Atmospheric Measurement Techniques
Open Access
Discussions

The Greenhouse Gas Climate Change Initiative (GHG-CCI): comparative validation of GHG-CCI SCIAMACHY/ENVISAT and TANSO-FTS/GOSAT CO_2 and CH_4 retrieval algorithm products with measurements from the TCCON network

B. Dils[1], M. Buchwitz[2], M. Reuter[2], O. Schneising[2], H. Boesch[3], R. Parker[3], S. Guerlet[4,*], I. Aben[4], T. Blumenstock[5], J. P. Burrows[2], A. Butz[5], N. M. Deutscher[2,7], C. Frankenberg[6], F. Hase[5], O. P. Hasekamp[4], J. Heymann[2], M. De Mazière[1], J. Notholt[2], R. Sussmann[5], T. Warneke[2], D. Griffith[7], V. Sherlock[8], and D. Wunch[9]

[1]Belgian Institute for Space Aeronomy (BIRA-IASB), Brussels, Belgium
[2]Institute of Environmental Physics (IUP), University of Bremen, Bremen, Germany

[3]University of Leicester, Leicester, UK
[4]SRON Netherlands Institute for Space Research, Utrecht, the Netherlands
[5]Karlsruhe Institute of Technology (KIT), Karlsruhe and Garmisch-Partenkirchen, Germany
[6]Jet Propulsion Laboratory (JPL), Pasadena, California, USA
[7]University of Wollongong, Australia
[8]National Institute of Water and Atmospheric Research (NIWA), Lauder, New Zealand
[9]California Institute of Technology, Pasadena, California, USA
[*]now at: Laboratoire de Météorologie Dynamique (LMD), Palaiseau, France

Received: 30 August 2013 – Accepted: 10 September 2013 – Published: 2 October 2013

Correspondence to: B. Dils (bart.dils@aeronomy.be)

Published by Copernicus Publications on behalf of the European Geosciences Union.

Abstract

Column-averaged dry-air mole fractions of carbon dioxide and methane have been retrieved from spectra acquired by the TANSO-FTS and SCIAMACHY instruments on board GOSAT and ENVISAT using a range of European retrieval algorithms. These retrievals have been compared with data from ground-based high-resolution Fourier Transform Spectrometers (FTS) from the Total Carbon Column Observing Network (TCCON). The participating algorithms are the Weighting Function Modified Differential Optical Absorption Spectroscopy (DOAS) algorithm (WFMD, University of Bremen), the Bremen Optimal Estimation DOAS algorithm (BESD, University of Bremen), the Iterative Maximum A Posteriori DOAS (IMAP, Jet Propulsion Laboratory (JPL) and Netherlands Institute for Space Research algorithm (SRON)), the proxy and full-physics versions of SRON's RemoTeC algorithm (SRPR and SRFP respectively) and the proxy and full-physics versions of the University of Leicester's adaptation of the OCO (Orbiting Carbon Observatory) algorithm (OCPR and OCFP respectively). The goal of this algorithm inter-comparison was to identify strengths and weaknesses of the various so-called Round Robin data sets generated with the various algorithms so as to determine which of the competing algorithms would proceed to the next round of the European Space Agency's (ESA) Greenhouse Gas Climate Change Initiative (GHG-CCI) project, which is the generation of the so-called Climate Research Data Package (CRDP), which is the first version of the Essential Climate Variable (ECV) "Greenhouse Gases" (GHG).

For CO_2, all algorithms reach the precision requirements for inverse modelling (< 8 ppb), with only WFMD having a lower precision (4.7 ppm) than the other algorithm products (2.4–2.5 ppm). When looking at the seasonal relative accuracy (SRA, variability of the bias in space and time), none of the algorithms have reached the demanding < 0.5 ppm threshold.

For CH_4, the precision for both SCIAMACHY products (50.2 ppb for IMAP and 76.4 ppb for WFMD) fail to meet the < 34 ppb threshold, but note that this work focusses

on the period after the 2005 SCIAMACHY detector degradation. The GOSAT XCH_4 precision ranges between 18.1 and 14.0 ppb. Looking at the SRA, all GOSAT algorithm products reach the < 10 ppm threshold (values ranging between 5.4 and 6.2 ppb). For SCIAMACHY, IMAP and WFMD have a SRA of 17.2 ppb and 10.5 ppb respectively.

1 Introduction

According to the IPCC 2007 report (Solomon et al., 2007), based on estimates of radiative forcing between 1750 and 2005, carbon dioxide and methane combined, account for over 80 % of the anthropogenic greenhouse gas warming effect. It is therefore important to understand the magnitude and distribution of the CO_2 and CH_4 sources and sinks. Despite their importance, our knowledge of the sources and sinks still has significant gaps (e.g. Stephens et al., 2007; Canadell et al., 2010). For instance it is still unclear why between ~ 2000 and 2006 methane levels in the atmosphere were rather stable (Simpson et al., 2012), while before and after this period they were rising (currently by about 7–8 ppb yr^{-1}, e.g. Rigby et al., 2008; Schneising et al., 2011).

Currently surface in situ trace gas concentration measurements are the primary data used to constrain inverse model estimates of surface fluxes (Baker et al., 2006), but these measurements only cover a fraction of earth's atmosphere. Global satellite observations, sensitive to the near-surface CO_2 and CH_4 variations, are therefore important datasets to improve these flux estimations (Chevallier et al., 2007; Bergamaschi et al., 2009). However given the long atmospheric lifetimes of both gases (30–95 yr for CO_2, ~ 12 yr for CH_4, e.g., Jacobson, 2005; Prather, 1994; Prather et al., 2001), the fluxes are small compared to the resident quantity in the atmosphere. Therefore the satellite accuracy requirements are very demanding, since small errors in the retrieved total column concentrations may result in significant errors in the derived fluxes (e.g., Meirink et al., 2006; Chevallier et al., 2007).

Currently only two satellite instruments, SCIAMACHY on board ENVISAT (Bovensmann et al., 1999) and TANSO-FTS on board GOSAT (Kuze et al., 2009), deliver, or

AMTD
6, 8679–8741, 2013
The Greenhouse Gas Climate Change Initiative (GHG-CCI)
B. Dils et al.

have delivered (SCIAMACHY operation ended in April 2012), measurements that are sensitive to near-surface CO_2 and CH_4 concentration variations. Both make use of the near-infrared/short-wave-infrared (NIR/SWIR) spectral region, to analyse the reflected solar radiation in a nadir looking configuration.

The aim of the European Space Agency's (ESA) Greenhouse Gas Climate Change Initiative (GHG-CCI) project is to provide a single high quality satellite product for each trace gas retrieval (four satellite-species combinations in total); the so-called Essential Climate Variables (ECVs). In the Round-Robin (RR) evaluation phase of the project, a number of different algorithms are competing to proceed into the next phase of the project, which is the development of the afore-mentioned ECV records. Here we will present the validation results of these algorithms, using retrievals from spectra acquired by ground-based high-resolution Fourier Transform Spectrometers (FTS) in the Total Carbon Column Observing Network (TCCON). All the algorithms discussed in this paper have already been validated to some extent at various stages in their development, often using the very same TCCON network data. However, approaches such as the collocation area and time, averaging of data over time etc. often vary between each study. Here we will present a comparative validation study, using a uniform strategy, focussing on the inter-algorithm differences and the significance thereof. The decision reached at the end of the Round-Robin analysis was based on more than this study alone. A general overview of the project's complete quality assessment results is given in Buchwitz et al. (2013).

2 Instruments

SCIAMACHY is a grating spectrometer on board the European environmental satellite ENVISAT, which was launched on 1 March 2002 into a sun synchronous polar orbit. After a decade in orbit, contact with the satellite was finally lost on the 8 April 2012. The SCIAMACHY instrument measured reflected, transmitted and backscattered solar radiation with a 0.2–1.4 nm resolution (Bovensmann et al., 1999). Its spectral band pass was divided into 8 channels. The first 6 covered the 214–1750 nm region while channels 7 and 8 covered the 1940–2040 nm and 2265–2380 nm intervals respectively. Unfortunately NIR/SWIR channels 7 and 8 suffered from in-flight ice deposition on the detector. Therefore, despite the fact that these channels featured many CO_2 and CH_4 absorption features, the retrieval algorithms discussed in this paper make use of channel 6. A problem of channel 6 is that the number of dead and bad detector pixels continued to increase in the spectral region used for methane retrieval during the instrument's lifetime.

The Greenhouse gas Observing SATellite (GOSAT) was launched on the 23 January 2009 by the Japanese Space Agency (JAXA) as a dedicated greenhouse gas monitoring satellite (Kuze et al., 2009). It is equipped with two instruments: TANSO-FTS, which stands for "Thermal And Near infrared Sensor for carbon Observations-Fourier Transform Spectrometer" and TANSO-CAI (a Cloud and Aerosol Imager that supports the FTS measurements). The TANSO-FTS instrument has four spectral bands with a resolution of 0.3 cm^{-1}, of which 3 operate in the SWIR (around 760, 1600 and 2000 nm) and one (between 5500–14 300 nm) in the thermal infrared. The first 3 provide sensitivity to the entire column including good near-surface sensitivity, while the latter is sensitive to the mid-troposphere.

ENVISAT/SCIAMACHY retrieval algorithms are typically associated with the instrument (i.e. SCIAMACHY), while GOSAT/TANSO-FTS algorithms typically use the satellite (i.e. GOSAT) identifier. For sake of consistency, we use the above mentioned convention in this paper. Therefore, if we refer to GOSAT, we are implying the TANSO-FTS instrument on board GOSAT.

3 Retrieval algorithms

In total, 10 retrieval algorithm products (listed in Table 1 together with their version number and appropriate references) have been compared in 4 separate comparison pools for the four ECVs, namely SCIAMACHY/XCH_4, SCIAMACHY/XCO_2, GOSAT/XCH_4

AMTD
6, 8679–8741, 2013

and GOSAT/XCO_2. The features of all algorithms have already been reported in several peer-reviewed publications, and in the GHG-CCI Algorithm Theoretical Basis Document (ATBD, Reuter et al., 2012), so we will only give a very brief overview. Several algorithms come in a full physics (typically tagged by FP in their four letter acronym) and proxy (PR) version. The proxy method uses a "reference gas" to derive the dry air column-averaged mole fraction (XCO_2 and XCH_4). This reference gas (in the case of CH_4, CO_2 is used as the reference, in the case of CO_2, O_2 is used) needs to have a far lower variability (in space and time) than the species of interest. This method allows for a very fast but still at least reasonably accurate retrieval in which many of the retrieval errors are cancelled in the CH_4/CO_2 or CO_2/O_2 ratio. On the downside, some error components do not cancel out and, in case of XCH_4, one needs to correct for the remaining variability of the CO_2 reference gas, typically by using a global model (see for instance Frankenberg et al., 2005, 2011; Parker et al., 2011; Schneising et al., 2009, 2011; Schepers et al., 2012). The full physics algorithms, on the other hand, model all relevant physical effects and derive the dry-air column-averaged mole fractions from the retrieved surface pressure or meteorological data. They are computationally more demanding than their proxy counterparts, but their dependence on models is reduced (Butz et al., 2011). All algorithms are still under continuous development, and indeed in some cases have already released an updated version (e.g. Guerlet et al., 2013; Oshchepkov et al., 2013). This paper deals with the versions submitted to the GHG-CCI Round Robin data pool.

3.1 SCIAMACHY XCO_2 algorithms

Here the Weighting Function Modified (WFM) Differential Optical Absorption Spectroscopy (DOAS) algorithm (henceforward referred to as WFMD) competes with The Bremen Optimal Estimation DOAS (BESD) algorithm, both developed at the University of Bremen. For WFMD we refer to Buchwitz et al. (2000, 2005, 2007), Schneising et al. (2008, 2009, 2011, 2012) and Heymann et al. (2012a). The version validated in this paper is described by Heymann et al. (2012b). For BESD, a more recent product, we refer to Reuter et al. (2010, 2011). WFMD is a proxy least-squares method based on a fast look-up table (LUT) scheme and uses a single constant atmospheric prior. BESD on the other hand is a full physics algorithm based on Optimal Estimation (Rodgers, 2000) and uses on-line radiative transfer (RT) model simulations. Note that WFMD is the only XCO_2 retrieval algorithm that did not feature a bias correction post-processing step based on TCCON (which would improve its validation parameters).

3.2 GOSAT XCO_2 algorithms

Here we have two Full Physics algorithms; one developed at the University of Leicester (UoL), referred in this article as OCFP, and one at SRON, the Netherlands Institute for Space Research, referred to as SRFP. The first is UoL's take on the OCO (Orbiting Carbon Observatory, Crisp et al., 2004) full physics algorithm (Cogan et al., 2012). The second is a development of SRON's RemoTeC algorithm (Butz et al., 2011). Both algorithms adjust parameters of a surface-atmosphere state vector and other parameters to the satellite observations, but differ in many other aspects such as their inversion scheme (optimal estimation vs. Tikhonov–Phillips), RT models, pre-and post-processing etc. For more information we refer to Cogan et al. (2012) and Butz et al. (2011). Note that both algorithms feature a post-processing bias-correction scheme. The algorithms are henceforward referred to as SRFC and OCFC.

3.3 SCIAMACHY XCH_4 algorithms

Again we have the WFMD algorithm, although this time the version described in Schneising et al. (2011) together with the IMAP (Iterative Maximum A Posteriori) DOAS (Frankenberg et al., 2011) algorithm (in this article further referred to as IMAP). Both algorithms are fairly mature but have primarily focused on the first three years of SCIAMACHY retrievals up till the 2005 SCIAMACHY detector degradation in the methane spectral region. Extending the time series beyond 2005 remains a challenge (see

AMTD
6, 8679–8741, 2013

Frankenberg et al., 2011, and Schneising et al., 2011, for details). Both are proxy algorithms.

3.4 GOSAT XCH_4 algorithms

Here we have both the full physics and proxy versions of the UoL (OCFP & OCPR) and SRON (SRFP & SRPR) algorithms mentioned above in Chapter 3.2. We refer to Parker et al. (2011) for information on OCFP and OCPR, to Butz et al. (2011) for SRFP and Schepers et al. (2012) for SRPR.

4 TCCON

The Total Carbon Column Observing Network (TCCON) (Wunch et al., 2011a) is a network of ground-based Fourier transform spectrometers (FTSs) that provide long and quasi-continuous timeseries of precise and accurate column abundances of CO_2, CH_4, N_2O and CO, retrieved from near-infrared (NIR) solar absorption spectra using a non-linear least-squares fitting algorithm called GFIT. Rather than retrieving the entire profile, GFIT scales an a priori profile to produce a synthetic spectrum that provides the best match with the measured spectrum. TCCON also makes use of the retrieved O_2 columns to derive the corresponding dry-air column averaged mole fractions.

$$XCO_2 = 0.2095(CO_2\text{column}/O_2\text{column}) \tag{1}$$

$$XCH_4 = 0.2095(CH_4\text{column}/O_2\text{column}) \tag{2}$$

Note that the TCCON O_2 retrieval uses the 1.27 micron band of O_2, not the O_2 A band used in satellite retrievals. An important aspect of TCCON is that aircraft measurements have been performed over many sites, which allow for an empirical scaling to calibrate the TCCON measurements to the WMO standard reference scale (Wunch et al., 2010; Deutscher et al., 2010; Geibel et al., 2012; Messerschmidt et al., 2012; Washenfelder et al., 2006). The scaling factor is uniform for all sites, 0.989 ± 0.001

AMTD
6, 8679–8741, 2013

(1σ) and 0.978 ± 0.002 for XCO_2 and XCH_4 respectively. The uncertainty on the TCCON/Aircraft ratio also yields information on the total (station-to-station) network consistency (1σ uncertainty of 0.4 ppm for XCO_2 and 3.5 ppb for XCH_4, see Wunch et al., 2010). The 10 TCCON stations employed in this study together with their coordinates and periods of operation are listed in Table 2. It is clear that not only the time at which these stations became operational differ, but also the amount of data obtained within a given time period. Because solar absorption FTS measurements can only be made under clear sky conditions, site location, and the corresponding occurrence of clear-sky days, has a large impact on the number of available measurements.

The TCCON data used in this paper were analysed with the GGG2012 version of the standard TCCON retrieval algorithm.

5 Methodology

The scope of the Round-Robin algorithm-TCCON comparisons was to identify any remaining short-comings in the data products generated with the competing algorithms and determine any inter-algorithm quality differences. Therefore the methodology has been kept straightforward and simple, but identical for all algorithms involved.

Complicating the validation is the fact that both TCCON and satellite measurements provide best estimates of the true atmospheric state, based on their own individual sensitivities and a priori information. According to Rodgers (2000), one can correct for the different a priori profiles used in the TCCON and satellite retrieval algorithms. Here we have opted to use the TCCON a priori as the common a priori profile for all measurements. Using Rodgers (2000):

$$x_{\mathrm{cor}} = x + \frac{1}{m_0}\sum_i m^i \left(A^i - 1\right)(\mathrm{ap}^i_x - \mathrm{ap}^i_T) \tag{3}$$

In which x_{cor} and x are the a priori-corrected and original column-averaged dry air mole fractions, i is the vertical layer index, m^i corresponds with the mass of dry air in layer

AMTD
6, 8679–8741, 2013
The Greenhouse Gas Climate Change Initiative (GHG-CCI)
B. Dils et al.

i, which is directly derived from $\Delta p^i/g^i$. Here Δp^i is the dry air pressure difference over layer i and g the gravitational constant. m_0 is the sum of m^i over all layers. A^i corresponds with the satellite algorithm's column averaging kernel, while ap_x and ap_T are the algorithm and TCCON a priori dry-air mole fractions in layer i respectively.

The impact of the a priori correction is fairly limited. For XCO_2, most algorithms exhibit a quasi-constant correction factor (a priori corrected-original) over all stations ranging between −0.68 and 0.63 ppm. Only WFMD exhibits a stronger and more erratic a priori correction, no doubt due to the single constant a priori it uses in its retrieval scheme (see Fig. 1). For XCH_4, we again notice a quasi-constant correction apart from OCFP and WFMD at Darwin and the SRON products at Lauder. OCFP uses an a priori, directly from the TM3 model, while for OCPR a stratospheric adjustment is made using GEOS-Chem model simulations, as the OCPR data exhibits a far smaller correction at Darwin compared to OCFP, an offset in the TM3 stratospheric output is probably the cause. SRON on the other hand uses a XCH_4 a priori derived from the TM4 model (Meirink et al., 2006).

Also noticeable in Fig. 2 is the gradual increase in the WFMD correction factor as we move from North to South, while the SRON products show a slight decrease (apart from Lauder). All the XCH_4 a priori corrections range between −8.6 and 13.7 ppb.

Note that we only corrected for the a priori difference and not for the difference in vertical sensitivity. That is, even with the same a priori profile its relative contribution to the end result still depends on the averaging kernels. Considering this aspect in the TCCON-satellite comparisons, both of which yield only total column information, requires a reasonable estimate of the true atmospheric variability, which is not available on a global scale. In Wunch et al. (2011b) a detailed assessment of this issue was made, comparing ACOS-GOSAT XCO_2 (O'Dell et al., 2012) with TCCON measurements. The study was limited to data taken at the Lamont station only, where the real atmospheric variability could be derived from regular aircraft observations. They found that smoothing the TCCON profile with the ACOS-GOSAT averaging kernel at Lamont induced a bias of about 0.6 ppm with no significant seasonal cycle or airmass dependence. The a priori correction on the other hand did feature a seasonal and latitudinal dependence, as expected, given that, contrary to the TCCON a priori, the ACOS a priori does not feature a seasonal cycle. No such evaluation has yet been made for a XCH_4 retrieval product, nor can it currently be made for any other station. With no ad hoc information on what best represents the true state for all stations, we limit ourselves to the a priori correction described above.

After the a priori-correction, all available timeseries have been trimmed so as to work, in each given comparison round, with data that have matching temporal coverage. For SCIAMACHY/XCH_4 this corresponds with 2003–2009, for SCIAMACHY/XCO_2: 2006–2009, and both GOSAT/XCO_2 and XCH_4 are limited to between April 2009 and April 2011.

As with every satellite vs. FTS comparison we defined a collocation time and area in which satellite and ground-based measurements can be paired. Ideally these criteria are as strict as possible in order to minimize the impact of spatial and temporal variability on the comparison. Here we have set the collocation time to ±2 h. The spatial collocation criterion was set at a 500 km radius around the TCCON site. Smaller collocation areas have been tested (100, 350 km) but often yielded unstable results, due to insufficient data. All FTS datapoints that fall within the temporal overlap criteria of a single satellite measurement (that fell in the spatial overlap area) are then averaged to obtain a unique satellite-FTS data pair.

The typical variability (1σ), including random errors and real atmospheric variability, of the FTS measurements within this 4 h overlap timeframe, is on average 2.5 ppb for XCH_4 and 0.4 ppm for XCO_2. Relaxing the overlap criteria does have a significant impact on the variability and at ±6 h the variability increases to 3.5 ppb (XCH_4) and 0.5 ppm (XCO_2).

From these data-pairs we derived various statistical parameters. In the figures and tables within this article, N corresponds to the number of collocated data pairs, R is the Pearson's r correlation coefficient, Bias is the average satellite-FTS difference:

$$\text{Bias} = \text{mean}(X_{\text{sat}} - X_{\text{FTS}}) \qquad (4)$$

Discussion Paper | Discussion Paper | Discussion Paper | Discussion Paper |

AMTD

6, 8679–8741, 2013

The Greenhouse Gas Climate Change Initiative (GHG-CCI)

B. Dils et al.

while the scatter corresponds with the standard deviation of said difference:

$$\text{Scatter} = \text{std}(X_{\text{sat}} - X_{\text{FTS}}) \tag{5}$$

Note that the single measurement precision requirements for inverse modelling, set forward by the users, is < 8 ppm for XCO_2 and < 34 ppb in case of XCH_4 (Buchwitz et al., 2011).

All these parameters have been calculated using the individual data-pairs as well as daily and monthly means. Note that both the daily and monthly means are derived from the individual data pairs, thus the ±2 h collocation criterion still applies. In the analysis all data pairs are considered to have equal weight. In this article we will show the results of the individual data pairs only, except for the correlation coefficient R, which is based on the daily averages. Also the time series plots shown are daily averages.

One of the important quality criteria put forward by the users is the so-called "relative accuracy". This parameter is an indication of the variability of the bias in space and time. The relative accuracy user requirements (1σ standard deviation) put forward by the inverse modelling community are 10 ppb for XCH_4 and 0.5 ppm for XCO_2 (Buchwitz et al., 2011) based on 1000 km^2 monthly averages. For inverse modelling purposes this parameter is more important than the overall bias as this, if consistent, can be easily corrected for. While this parameter cannot be exactly replicated in our analysis, we calculate a so-called "relative accuracy" (RA), which attempts to yield some information on the station to station variability of the bias. We define RA as the standard deviation on the overall biases (derived from individual data) obtained at each station.

The "seasonal relative accuracy" (SRA) is the standard deviation over all seasonal bias results (40 in total, 4 seasonal biases over 10 stations). The seasonal bias results for each station are constructed from all datapairs which fall within the months of January to March (JFM), April to June (AMJ), July to September (JAS) or October to December (OND), regardless of the year the measurements are taken. Some stations feature only limited data during certain seasons, which sometimes results in erratic bias results. To avoid the inclusion of these results into the RA and SRA calculation, we do not include those bias results that are derived from fewer than 10 individual datapoints or have a standard error ($\sigma/\sqrt{N}$) which exceeds the user relative accuracy requirements (0.5 ppm XCO_2, 10 ppb XCH_4). RA and SRA are also derived from a common dataset, thus if one algorithm in the validation round fails to meet the quality requirements for station x and season y, the corresponding bias result is also excluded from the SRA and RA calculation of its competitor.

In case all 4 seasonal biases for a station meet the quality requirements, we also derive the standard deviation on these four results as an indicator of their variability. This parameter is referred to as the "seasonality" (Seas).

6 Results

Shown in each section are overview figures (4, 7, 10 and 13) and tables (3 till 12) that list the statistical parameters obtained at each station, and for all station data combined (ALL). Given the uneven distribution of data among the 10 TCCON stations, stations with high data density such as Lamont have a higher impact on the "all data" results. For practical purposes we will only show an example timeseries of a single European, North American and Oceanian station.

The overview Tables 13 and 14 also list the 95 % confidence interval of the overall parameters. The confidence intervals on the scatter, RA, Seas and SRA are inferred from the Chi squared (χ^2) distribution in which

$$\sqrt{\frac{(N-1)\,s^2}{\chi^2_{(\frac{\alpha}{2},N-1)}}} \leq \sigma \leq \sqrt{\frac{(N-1)\,s^2}{\chi^2_{(1-\frac{\alpha}{2},N-1)}}} \tag{6}$$

with σ the population standard deviation, s the sample standard deviation, N the number of data points in the sample and α, determining the confidence level (here 0.05 for 95 % confidence).

Discussion Paper | Discussion Paper | Discussion Paper | Discussion Paper |
AMTD
6, 8679–8741, 2013
The Greenhouse Gas Climate Change Initiative (GHG-CCI)
B. Dils et al.

We also performed a so-called F test, to quantify the probability that the statistical parameters of two competing results stem from the same population (Snedecor and Cochran, 1989). The null Hypothesis (H_0) of the test states that the variances of the two populations are equal ($\sigma_1^2 = \sigma_2^2$). The result of the test is the probability that the stated hypothesis is true. Thus, the lower this number, the more likely it is that the obtained parameters such as RA and SRA of two competing algorithms are different.

Note that the F test relies on the presumption that the population exhibits a normal distribution. One could invoke the central limit theorem as the data from which the RA, Seas and SRA are drawn are sample means from the overall population. However, the sampling itself can hardly be called random. Thus to test for normality, we performed a Shapiro–Wilk Normality test (Shapiro and Wilk, 1965), on a 0.05 confidence level, on all the relevant data samples. All data samples passed the test apart from the SRA samples from OCPR XCH_4 and BESD XCO_2. We also plotted the Quantile–Quantile probability (Q–Q plot) and found no clear departure from linearity in any dataset. Figure 3 shows the Q–Q results for the BESD XCO_2 and OCPR XCH_4 SRA data. For BESD, despite its failed Shapiro–Wilk test, no strong deviations from linearity are observed apart from the tails (which is commonly observed in Q–Q plots). OCPR appears much more erratic, with a significant departure around 0 theoretical quantile. However there is no indication of any smooth curved deviation from linearity either.

6.1 SCIAMACHY XCO_2

The two competing algorithms are BESD and WFMD. Table 3 and Fig. 4a shows the evolution of the bias over the different stations, the error bars in Fig. 4a correspond to the 95 % confidence bands of the bias. Note that there is no data for Karlsruhe since the TCCON measurements there commenced in 2010, while there were no post 2009 WFMD data at the time of this analysis. The overall bias is slightly smaller for BESD but the variability of the bias (i.e. relative accuracy) is almost identical (1.28 vs. 1.29 ppm).

The most significant differences between both datasets are the scatter and data density (Fig. 4b and d). While the overall scatter for BESD is significantly lower (2.5 ppm

AMTD
6, 8679–8741, 2013

vs. 4.7 ppm for WFMD), its data density is also lower (9674 vs. 31 818 data pairs). Interestingly this makes the uncertainty on the overall bias i.e. the standard error ($\sigma/\sqrt{N}$) very similar (0.025 vs. 0.026 ppm for BESD and WFMD respectively). The higher scatter for WFMD also reveals itself in the generally lower correlation coefficients. Note that for the Lauder station, situated in New Zealand, BESD only offers 3 data pairs, all of which are measured on the same day (hence the lack of a daily correlation coefficient for this station). Both algorithms fail the above stated quality requirements at this site and if we thus exclude the Lauder station from our analysis, the relative accuracy (RA in the Table) of BESD improves to 0.63 ppm, while that of WFMD (slightly) deteriorates to 1.36 ppm.

The timeseries in Figs. 5 (BESD) and 6 (WFMD) are collocated daily averaged FTS and satellite measurements from Bialystok (a), Lamont (b) and Darwin (c) respectively. Comparing these figures, it is clear that BESD features substantially less data than WFMD. Also clearly visible is the extremely limited (if any) seasonal cycle in the Darwin data. BESD data clearly exhibits lower scatter but some outliers can be identified. This has been identified as an issue related to the SCIAMACHY Level 1 version 7 consolidation product (L1v7u), used in the retrieval. Tests with the new L1v7w data show that these outliers are eliminated, which should further increase BESD's precision.

The seasonality of Lamont, Darwin and the overall results are slightly in favour of BESD as well as the SRA value (see Table 4). Keep in mind however that these parameters are derived from a limited data sample. Neither the seasonality, nor SRA difference is significant (P value of the H_0: $\sigma_1^2 = \sigma_2^2$, or the probability that both samples are from a population with equal variances, is 0.55 and 0.42 respectively). The P value for the RA H_0: $\sigma_1^2 = \sigma_2^2$ hypothesis on the other hand is 0.06.

6.2 GOSAT $X\mathbf{CO_2}$

Here we have two competing algorithms. OCFC and SRFC, which are the full physics, bias corrected, versions of University of Leicester's OCO and SRON's RemoteC algorithms respectively.

As one can see in Fig. 7 and Tables 5 and 6, the differences concerning all parameters are extremely small. Number of datapoints, scatter and correlation coefficients are never consistently in favour of one algorithm. Note that the correlation coefficients are quite low for the Southern Hemisphere stations of Darwin, Wollongong and Lauder, which is attributed to the limited seasonal XCO_2 variability at these sites. The relative accuracy (RA) is slightly in favour of OCFC (0.64 vs. 0.84 ppm for SRFC). Again we have a large uncertainty on the bias values for Lauder. Excluding this station from the relative accuracy calculation, yields an RA equal to 0.53 and 0.74 ppm for OCFC and SRFC respectively. The probability that both sample RA values stem from an equal distribution is 0.32.

Looking at the timeseries for Orleans, Lamont and Wollongong, (Figs. 8 and 9) there is hardly any difference between the two algorithms. However, OCFC does feature several strong outliers in all 3 stations. Unlike the station to station bias variability, SRFC has a lower variability in the overall seasonal bias (see Table 6). For both algorithms the winter-autumn (October till March) biases seem to be more negative than their spring-summer counterparts. This is also the case for the BESD algorithm. While the difference in overall seasonality (0.74 for OCFC vs. 0.33 for SRFC) is somewhat distinct ($P(H_0\!: \sigma_1^2 = \sigma_2^2)$ is 0.22), the difference in SRA (1.08 for OCFC vs. 0.89 for SRFC) is very small ($P(H_0\!: \sigma_1^2 = \sigma_2^2)$ is 0.68).

6.3 SCIAMACHY XCH_4

Both IMAP and WFMD are fairly mature proxy type algorithms. Note however that since November 2005 the SCIAMACHY XCH_4 retrievals suffered from a detector degradation in Channel 6. Most of the TCCON stations (apart from Park Falls, Darwin and Lauder) commenced their measurements after this event. The quality assessment in this paper is therefore primarily representative of this post decay period.

We also have to note that during the course of the validation, we detected strong biases in the January till March IMAP seasonal values. This turned out to be a processing error in IMAP (one of the clusters used incorrect settings from a previous IMAP run). All

AMTD
6, 8679–8741, 2013

the data derived from that processing unit have been removed from the IMAP dataset. This reduced the amount of overlapping data from 55 626 to 42 320 (or almost 24 %).

The differences between the algorithms are fairly distinctive (see Fig. 10 and Table 7). Obvious is the far larger scatter (see Fig. 10b) in the WFMD data (overall 76 ppb compared to 50 ppb for IMAP). This also translates in an inferior correlation coefficient over all stations except for Wollongong (which features a negative correlation for both algorithms) and Bremen (by a very small amount). Unlike the BESD-WFMD XCO_2 comparison, WFMD's higher scatter properties are not offset by a superior data density. So on these parameters alone IMAP seems to outperform WFMD. The reason for the larger scatter of the WFMD data is likely due to the fact that WFMD is based on unconstrained linear least-squares using a single constant methane a priori profile whereas IMAP is based on Optimal Estimation using methane model data as a priori information. In addition, there are also other reasons which can explain the differences. For example, IMAP and WFMD differ greatly in their pre-processing steps, targeted at dealing with the problematic SCIAMACHY instrument degradation. IMAP, for instance, uses SRON's own specifically calibrated input spectra, while WFMD uses the official standard SCIAMACHY level 1 data. IMAP uses one single pixel filter (the so-called "Dead and Bad detector Pixel Mask" or DBPM), while WFMD uses several masks, each one optimized for a certain time period.

However looking at the bias distribution, all three Southern Hemisphere stations (Darwin, Wollongong and Lauder) exhibit a considerable negative bias. Also for WFMD, these three stations feature a more negative bias than their Northern Hemisphere counterparts but not as distinctive as for IMAP. For IMAP the difference between the mean Southern and Northern Hemisphere bias is 26 ppb, while for WFMD it is 13 ppb. This also reflects itself in the relative accuracy which is 7.8 ppb for WFMD and 14.7 ppb for IMAP.

Given the large scatter, it is difficult to assess any systematic seasonality errors in the timeseries plots (see Figs. 11 and 12). The IMAP underestimation at Darwin is clear, as well as the stronger scatter in WFMD. Table 8 lists the overall seasonal biases. As with the RA, we see a higher SRA in the IMAP data, although the difference is far less distinctive. For RA $P(H_0: \sigma_1^2 = \sigma_2^2)$ is 0.09, while for SRA $P(H_0: \sigma_1^2 = \sigma_2^2)$ equals 0.28. The difference in overall seasonality (4.0 for IMAP vs. 6.6 for WFMD) is even less significant ($P(H_0: \sigma_1^2 = \sigma_2^2) = 0.43$).

6.4 GOSAT XCH_4

Concerning the bias (see Fig. 13, and Tables 9 and 10), as with SCIAMACHY XCH_4, the Southern Hemisphere bias values tend to be somewhat lower (in absolute values) than their Northern Hemisphere counterparts, although only consistently so for SRPR and OCFP. The average Northern Hemisphere–Southern Hemisphere bias difference is 3.3 ppb for OCPR, 8.8 ppb for OCFP, 11.0 ppb for SRPR and 6.7 ppb for SRFP, all of which are considerably lower than that observed in IMAP (26 ppb). This is also reflected in the relative accuracy (RA) numbers, which range from 2.7 ppb (for OCPR) to 6 ppb (OCFP) (see Tables 9 to 10). The overall bias values themselves range from −2.5 (SRFP) to 7 ppb (OCPR).

Only OCFP has a somewhat lower precision (18.1 ppb), while the overall scatter of the other algorithms ranges between 14 and 14.9 ppb. None of the algorithms is consistently better or worse across all stations involved though (see Fig. 13 and Tables 9 and 10). Similar observations can be made about the correlation coefficients where each algorithm comes out with the best R value at, at least, one station (see Fig. 13c). OCFP has the worst overall scatter, correlation and relative accuracy of all the algorithms involved, while OCPR has the best scatter, data density, relative accuracy and correlation results (the latter a tie with SRPR). The difference between the best (OCPR = 2.7 ppb) and worst (OCFP = 6 ppb) relative accuracy result is significant on a 95 % level ($P(H_0: \sigma_1^2 = \sigma_2^2) = 0.03$). However the difference between the two best results (OCPR and SRFP at 3 ppb), clearly is not ($P(H_0: \sigma_1^2 = \sigma_2^2) = 0.76$). The two SRON RA values have a $P(H_0: \sigma_1^2 = \sigma_2^2) = 0.33$.

Discussion Paper | Discussion Paper | Discussion Paper | Discussion Paper |

AMTD
6, 8679–8741, 2013

The Greenhouse Gas Climate Change Initiative (GHG-CCI)

B. Dils et al.

Title Page
Abstract | Introduction
Conclusions | References
Tables | Figures
◂ | ▸
Back | Close
Full Screen / Esc
Printer-friendly Version
Interactive Discussion

The strong difference between the Leicester algorithms can be attributed to the fact that the full physics version of Leicester's OCO algorithm is a more recent development than its more mature proxy counterpart.

Turning to the seasonality, the full physics algorithms outperform their respective proxy counterparts by a small margin. Interestingly OCPR, which so far featured the best overall statistics, performs worst when looking at the seasonality. This is also somewhat evident from the timeseries plot (Fig. 14) where OCPR seems to underestimate the XCH_4 seasonal amplitude (obvious in Lamont). The differences between the other algorithms are less obvious (Figs. 15 to 17). Of course, being a proxy algorithm, some of the effects might come from the model used in the dry air conversion (i.e. CarbonTracker CT2010, Peters et al., 2007). SRFP has the best seasonality, keeping in mind that difference between the OCPR and SRFP seasonality is not conclusive ($P(H_0\text{: } \sigma_1^2 = \sigma_2^2) = 0.18$).

All seasonal relative accuracy (SRA) values range between 5.4 and 6.2 and no inter-algorithm difference is significant in this aspect (lowest $P(H_0\text{: } \sigma_1^2 = \sigma_2^2) = 0.45$)

7 Summary

Tables 13 and 14 list the overview results using all combined data as well as their 0.95 confidence intervals and the equal variance hypothesis probabilities. The results in Table 13 correspond with the overall (ALL) results in Tables 3, 5, 7 and 9. The reported errors are also derived from this complete dataset (using all available datapairs). Keep in mind that the station-to-station range in bias, scatter and correlation often far exceed the error boundaries in Table 13. That said, looking at Table 13, we see that distinctive differences between algorithms do exist, however Table 14, which features the analysis results of the inter-station and seasonal variability is far more ambiguous. This is of course a direct result of the sample data size. Table 13's results are derived from the individual data pairs, while Table 14's sample consists of the (seasonal) bias means. Only one inter-algorithm difference parameter reached the 0.95 confidence level (the

AMTD
6, 8679–8741, 2013

RA results between OCPR and OCFP XCH_4). Of all the H_0 probability values (P), only three parameters reach 0.9, four 0.8 and seven parameters a 0.68 confidence level ($\sim 1\sigma$) out of the 18 listed in Table 14. Also, the inter-algorithm differences between RA values are more significant than those of seasonality and SRA, even though the latter is probably the best quality estimator of what the users have defined as the relative accuracy. To remedy this ambiguity, one would need to increase the number of sample data. One way would be to use monthly instead of seasonal means. However this would greatly increase the number of unstable samples (due to the limited amount of correlative data from which these averages are constructed). This could also be improved by using different collocation criteria such as proposed by Keppel-Aleks et al. (2011), which was not feasible due to practical considerations. The most desirable option would be to expand the TCCON network. Note however that, for instance, to reach 0.95 confidence in the SRA difference between BESD and WFMD XCO_2 (1.19 vs 1.43 ppm), one would need 115 data samples (currently 21). Alternatively, with a perfect sample size of 40 (4 seasons × 10 stations), we can currently only distinguish, with 95 % accuracy, an SRA of 0.5 ppm (the threshold XCO_2 quality) with that of 0.68 ppm. With our best actual samples size (31) the latter becomes 0.72 ppm.

Note also that in the case of XCO_2 none of the algorithms' RA or SRA values reach said Relative Accuracy threshold value of 0.5 ppm as set forward by the users, nor do the SRA 95 % confidence bands encompass this value. What we obtain is the combined TCCON-Satellite accuracy and according to Wunch et al. (2010) the current TCCON XCO_2 network accuracy (1σ, station-to-station) is 0.4 ppm. Adding additional uncertainty due to collocation and smoothing errors, and the above mentioned uncertainty on the analysis itself, leaves little room for an accurate assessment of such a demanding threshold value for inverse modelling purposes. Efforts to decrease the station-to-station biases between TCCON stations are thus desirable and on-going. For XCH_4, SRA reaches the 10 ppb user quality threshold for all GOSAT algorithms, while SCIAMACHY WFMD's SRA approaches this number (10.5). IMAP would probably also meet this threshold if not for the Southern Hemisphere bias.

AMTD
6, 8679–8741, 2013

Even taking into account these uncertainties, at least in certain comparison rounds, the differences between the algorithm products were distinct enough to draw binding conclusions as to which one would proceed into the next round of the GHG-CCI project. Again it must be stressed that the decisions reached were not based on the comparisons with TCCON alone (see Buchwitz et al., 2013).

In the case of SCIAMACHY XCO_2, we see that BESD has a superior bias, scatter and correlation compared to WFMD. It's RA, Seas and SRA values are also consistently better, however only the RA with reasonable confidence ($P(H_0: \sigma_1^2 = \sigma_2^2) = 0.06$). So in this round the conclusion was to proceed with BESD.

The GOSAT XCO_2 comparisons on the other hand yielded no clear winner. Both have comparable scatter and correlation values (in fact using different collocation criteria yielded different winners in this category). OCFC's RA value is slightly better while its seasonality and SRA is slightly worse. Neither of these parameters is distinctive. As discussed in Buchwitz et al. (2013) global analysis of the data does yield, contrary to the TCCON locations, significant inter-algorithm differences. Certainly in areas with high (e.g. Saharan desert) or low (e.g. Amazon forest) surface albedo, which are not covered by TCCON, differences become significant (Guerlet et al., 2013). This observation triggered the development of a new algorithm which uses ensemble medians called the EnseMble Median Algorithm (EMMA, see Reuter et al., 2012). While the EMMA algorithm might be the best solution at hand, it does not negate the pressing need for expanding the TCCON network into key areas, enlarging the surface albedo range and geographical distribution of the network.

The SCIAMACHY XCH_4, comparisons between IMAP and WFMD, showed that in many aspects IMAP was the best performing algorithm (scatter, data density, correlation). However the inter-station bias difference, certainly between the northern and Southern Hemisphere, appears to be large. This results in an inferior RA and SRA value (although the statistical certainty of the latter parameter is far less distinct, and the RA difference reaches a 0.9 confidence level only). WFMD also shows an inter-hemispheric bias difference, only less significant. Also neither of the algorithms reach

Discussion Paper | Discussion Paper | Discussion Paper | Discussion Paper |

AMTD

6, 8679–8741, 2013

The Greenhouse Gas Climate Change Initiative (GHG-CCI)

B. Dils et al.

the threshold single observation precision (< 34 ppb), set forward by the users. Since these issues need to be resolved first, both algorithms proceeded to the next round. In this context it needs to be pointed out that the validation results presented here are dominated by data generated after 2005 where SCIAMACHY suffered from proceeding detector degradation in the spectral region used for methane retrieval. The results presented here are therefore not representative for the time period 2005 and earlier years, where the quality of the SCIAMACHY methane retrievals is much better (e.g., Buchwitz et al., 2013, and references given therein).

For GOSAT XCH_4, it's the less mature OCFP algorithm that stands out in a negative way. It has distinctively more scatter, a lower correlation coefficient and its RA value is distinctly worse than its proxy OCPR counterpart. OCPR on the other hand has the lowest scatter and highest data density, as well as the lowest RA value (although hardly distinct from its SRFP competitor). Neither of the algorithms, including OCFP, have a distinct SRA value. The margin in which OCPR stands out from its SRON competitors is however very small and in terms of seasonality it seems to perform worse (although with a 0.18 $P(H_0\colon \sigma_1^2 = \sigma_2^2)$, only with little more than 80 % certainty). Given this small margin and the fact that the comparison between the proxy and full physics SRON products show that the full physics method is a viable option, it was decided to proceed with both OCPR and SRFP.

8 Conclusions

We have analysed 10 retrieval products produced by the BESD, WFM-DOAS, IMAP-DOAS, RemoTeC and Leicester OCO algorithms. We focussed specifically on the inter-product differences. It was found that for SCIAMACHY (both XCO_2 and XCH_4), the competing algorithms yielded significantly different products; especially in terms of single measurement precision (i.e. scatter). In both XCO_2 and XCH_4, WFMD featured higher scatter than its competitor, being BESD for XCO_2 and IMAP for XCH_4. The latter on the other hand seems to suffer (more) from a significant northern vs. Southern

Hemisphere bias, an issue which requires more analysis. One reason for the larger scatter of the WFMD data product is that WFMD is based on unconstrained linear least-squares whereas BESD and IMAP are based on optimal estimation. However, there are several other retrieval properties, e.g., meteorological profiles, cloud filtering, consideration of light scattering, which influence the retrieval scatter.

Differences between all the competing GOSAT products are far less striking. For XCH_4, apart from the full physics version of Leicester's OCO algorithm (OCFP), the other algorithms (OCPR and SRON's RemoTeC full physics (SRFP) and proxy (SRPR) products) are very alike. In terms of precision, the proxy versions, especially OCPR, seem to have a slight edge, but in terms of inter-station bias variability and capturing the seasonal cycle, the SRON full physics algorithm is more than competitive. In fact there are indications that OCPR underestimates the XCH_4, but this might be due to the CarbonTracker CT2010 model (Peters et al., 2007) used in the dry air conversion instead of the proxy algorithm itself. For XCO_2, the competing products are closer still. Differences are small for all obtained statistical parameters, and no one algorithm betters the others across the board. This does not imply that these products feature no differences at all. In some regions (e.g. South-America, Africa, China) differences between algorithms can be substantial, but there is no TCCON data available in these regions to discriminate between algorithm performance (Buchwitz et al., 2013; Reuter et al., 2012).

The relative accuracy and single precision threshold quality criteria for inverse modelling (10 ppb and 34 ppb XCH_4 respectively) have been reached by all GOSAT XCH_4 products, and if the inter-hemispheric bias difference is mitigated (in a future version of the product or by using in situ data, see Bergamachi et al., 2009), so will, for the relative accuracy, in all likelihood, the SCIAMACHY XCH_4 products. However both IMAP and WFMD XCH_4 still do not reach the precision user requirement. In this context it needs to be pointed out that the validation results presented here are dominated by data generated after 2005 where SCIAMACHY suffered from proceeding detector degradation in the spectral region used for methane retrieval. The results presented

AMTD
6, 8679–8741, 2013

here are therefore not representative for the time period 2005 and earlier years, where the quality of the SCIAMACHY methane retrievals is much better (e.g., Buchwitz et al., 2013, and references given therein).

For XCO_2, all algorithms reach the single observation precision threshold (8 ppm), but none of the algorithms meet the relative accuracy user requirement (0.5 ppm). Unfortunately, given the current constellation of TCCON measurements, the assessment of whether an algorithm product has indeed reached this demanding value contains considerable uncertainty by itself. An expansion of the TCCON network into key geographic areas and efforts to even further reduce the TCCON station-to-station biases would be most welcome in this respect.

Acknowledgements. This work was primarily funded by ESA/ESRIN (GHG-CCI), with additional funds from EU FP7 (grant agreement No. 283576, MACC-II), DLR (SADOS), the State and the University of Bremen and PRODEX SECPEA/A3C. We thank the members of the GOSAT Project (JAXA, NIES, and Ministry of the Environment (MoE), Japan) for providing GOSAT Level 1B and Level 2 data products (GOSAT RA1PI project CONSCIGO). We also thank TCCON and related funding organizations (NASA grants NNX11AG01G, NAG5-12247, NNG05-GD07G, NASA Orbiting Carbon Observatory Program, DOE ARM program, the Australian Research Council, DP0879468 and LP0562346, the EU projects IMECC, InGoS and GEOmon, the Senate of Bremen).

References

Baker, D. F., Law, R. M., Gurney, K. R., Rayner, P., Peylin, P., Denning, A. S., Bousquet, P., Bruhwiler, L., Chen, Y.-H., Ciais, P., Fung, I. Y., Heimann, M., John, J., Maki, T., Maksyutov, S., Masarie, K., Prather, M., Pak, B., Taguchi, S., and Zhu, Z.: TransCom 3 inversion intercomparison: Impact oftransport model errors on the interannual variability of regional CO_2 fluxes, 1988–2003, Global Biogeochem. Cy., 20, GB1002, doi:10.1029/2004GB002439, 2006.

Bergamaschi, P., Frankenberg, C., Meirink, J. F., Krol, M., Villani, M. G., Houweling, S., Dentener, F., Dlugokencky, E. J., Miller, J. B., Gatti, L. V., Engel, A., and Levin, I.: Inverse modeling of global and regional CH_4 emissions using SCIAMACHY satellite retrievals, J. Geophys. Res., 114, D22301, doi:10.1029/2009JD012287, 2009.

Bovensmann, H., Burrows, J. P., Buchwitz, M., Frerick, J., Noël, S., Rozanov, V. V., Chance, K. V., and Goede, A. H. P.: SCIAMACHY – Mission objectives and measurement modes, J. Atmos. Sci., 56, 127–150, 1999.

Buchwitz, M., Rozanov, V. V., and Burrows, J. P.: A near-infrared optimized DOAS method for the fast global retrieval of atmospheric CH_4, CO, CO_2, H_2O, and N_2O total column amounts from SCIAMACHY Envisat-1 nadir radiances, J. Geophys. Res., 105, 15231–15245, 2000.

Buchwitz, M., de Beek, R., Burrows, J. P., Bovensmann, H., Warneke, T., Notholt, J., Meirink, J. F., Goede, A. P. H., Bergamaschi, P., Körner, S., Heimann, M., and Schulz, A.: Atmospheric methane and carbon dioxide from SCIAMACHY satellite data: initial comparison with chemistry and transport models, Atmos. Chem. Phys., 5, 941–962, doi:10.5194/acp-5-941-2005, 2005.

Buchwitz, M., Schneising, O., Burrows, J. P., Bovensmann, H., Reuter, M., and Notholt, J.: First direct observation of the atmospheric CO_2 year-to-year increase from space, Atmos. Chem. Phys., 7, 4249–4256, doi:10.5194/acp-7-4249-2007, 2007.

Buchwitz, M., Chevallier, F., and Bergamaschi, P.: User Requirements Document (URD) for the GHG-CCI project of ESA's Climate Change Initiative, Technical Report, pp. 45, version 1 (URDv1), 3 February 2011, available at: http://www.esa-ghg-cci.org (last access date: 1 October 2013), 2011.

Buchwitz, M., Reuter, M., Schneising, O., Boesch, H., Guerlet, S., Dils, B., Aben, I., Armante, R., Bergamaschi, P., Blumenstock, T., Bovensmann, H., Brunner, D., Buchmann, B., Burrows, J. P., Butz, A.,Chédin, A., Chevallier, F., Crevoisier, C. D., Deutscher, N. M., Frankenberg, C., Hase, F., Hasekamp, O. P., Heymann, J., Kaminski, T., Laeng, A., Lichtenberg, G., De Mazière, M., Noël, S., Notholt, J. Orphal, J., Popp, C., Parker, R., Scholze, M., Sussmann, R., Stiller, G. P., Warneke, T., Zehner, C., Bril, A., Crisp, D., Griffith, D. W. T.,Kuze, A., O'Dell, C., Oshchepkov, S., Sherlock, V., Suto, H., Wennberg, P., Wunch, D., Yokota, T., and Yoshida, Y.: The Greenhouse Gas Climate Change Initiative (GHG-CCI): comparison and quality assessment of near-surface-sensitive satellite-derived CO_2 and CH_4 global data sets, Remote Sens. Environ., in press, 2013.

Butz, A., Guerlet, S., Hasekamp, O., Schepers, D., Galli, A., Aben, I., Frankenberg, C., Hartmann, J.-M., Tran, H., Kuze, A., Keppel-Aleks, G., Toon, G., Wunch, D., Wennberg, P., Deutscher, N., Griffith, D., Macatangay, R., Messerschmidt, J., Notholt, J., and Warneke, T.: Towards accurate CO_2 and CH_4 observations from GOSAT, Geophys. Res. Lett., 38, L14812, doi:10.1029/2011GL047888, 2011.

Canadell, J. G., Ciais, P., Dhakal, S., Dolman, H., Friedlingstein, P., Gurney, K. R, Held, A., Jackson, R. B., Le Quéré, C., Malone, E. L., Ojima, D. S., Patwardhan, A., Peters, G. P., and Raupach, M. R.: Interactions of the carbon cycle, human activity, and the climate system: a research portfolio, Current Opinion in Environmental Sustainability, 2, 301–311, 2010.

Chevallier, F., Engelen, R. J., and Peylin, P.: The contribution of AIRS data to the estimation of CO_2 sources and sinks, Geophys. Res. Lett., 32, L23801, doi:10.1029/2005GL024229, 2005.

Chevallier, F., Bréon, F.-M., and Rayner, P. J.: Contribution of the Orbiting Carbon Observatory to the estimation of CO_2 sources and sinks: theoretical study in a variational data assimilation framework, J. Geophys. Res., 112, D09307, doi:10.1029/2006JD007375, 2007.

Cogan, A. J., Boesch, H, Parker, R. J., Feng, L., Palmer, P. I., Blavier, J.-F. L., Deutscher, N. M., Macatangay, R., Notholt, J., Roehl, C., Warneke, T., and Wunch, D.: Atmospheric carbon dioxide retrieved from the Greenhouse gases Observing SATellite (GOSAT): comparison with ground-based TCCON observations and GEOS-Chem model calculations, J. Geophys. Res., 117, D21301, doi:10.1029/2012JD018087, 2012.

Crisp, D., Atlas, R. M., Bréon, F.-M., Brown, L. R., Burrows, J. P., Ciais, P., Connor, B. J., Doney, S. C., Fung, I. Y., Jacob, D. J., Miller, C. E., O'Brien, D., Pawson, S., Randerson, J. T., Rayner, P., Salawitch, R. S., Sander, S. P., Sen, B., Stephens, G. L., Tans, P. P., Toon, G. C.,Wennberg, P. O., Wofsy, S. C., Yung, Y. L., Kuang, Z., Chudasama, B., Sprague, G., Weiss, P., Pollock, R., Kenyon, D., and Schroll, S.: The Orbiting Carbon Observatory (OCO) mission, Adv. Space Res., 34, 700–709, 2004.

Deutscher, N. M., Griffith, D. W. T., Bryant, G. W., Wennberg, P. O., Toon, G. C., Washenfelder, R. A., Keppel-Aleks, G., Wunch, D., Yavin, Y., Allen, N. T., Blavier, J.-F., Jiménez, R., Daube, B. C., Bright, A. V., Matross, D. M., Wofsy, S. C., and Park, S.: Total column CO_2 measurements at Darwin, Australia – site description and calibration against in situ aircraft profiles, Atmos. Meas. Tech., 3, 947–958, doi:10.5194/amt-3-947-2010, 2010.

Dlugokencky, E. J., Bruhwiler, L., White, J. W. C., Emmons, L. K., Novelli, P. C., Montzka, S. A., Masarie, K. A., Lang, P. M., Crotwell, A. M., Miller, J. B., and Gatti, L. V.: Observational constraints on recent increases in the atmospheric CH_4 burden, Geophys. Res. Lett., 36, L18803, doi:10.1029/2009GL039780, 2009.

Frankenberg, C., Meirink, J. F., van Weele, M., Platt, U., and Wagner, T.: Assessing methane emissions from global spaceborne observations, Science, 308, 1010–1014, 2005.

Frankenberg, C., Aben, I., Bergamaschi, P., Dlugokencky, E. J., van Hees, R., Houweling, S., van der Meer, P., Snel, R., and Tol, P.: Global column-averaged methane mixing ratios from 2003 to 2009 as derived from SCIAMACHY: trends and variability, J. Geophys. Res., 116, D04302, doi:10.1029/2010JD014849, 2011.

Geibel, M. C., Messerschmidt, J., Gerbig, C., Blumenstock, T., Chen, H., Hase, F., Kolle, O., Lavrič, J. V., Notholt, J., Palm, M., Rettinger, M., Schmidt, M., Sussmann, R., Warneke, T., and Feist, D. G.: Calibration of column-averaged CH_4 over European TCCON FTS sites with airborne in-situ measurements, Atmos. Chem. Phys., 12, 8763–8775, doi:10.5194/acp-12-8763-2012, 2012.

Guerlet, S., Butz, A., Schepers, D., Basu, S., Hasekamp, O. P., Kuze, A., Yokota, T., Blavier, J.-F., Deutscher, N. M., Griffith, D. W. T.,Hase, F.,Kyro, E.,Morino, I., Sherlock, V., Sussmann, R., Galli, A., and Aben, I.: Impact of aerosol and thin cirrus on retrieving and validating XCO_2 from GOSAT shortwave infrared measurements, J. Geophys. Res. Atmos., 118, 2169–8996, doi:10.1002/jgrd.50332, 2013.

Heymann, J., Schneising, O., Reuter, M., Buchwitz, M., Rozanov, V. V., Velazco, V. A., Bovensmann, H., and Burrows, J. P.: SCIAMACHY WFM-DOAS XCO_2: comparison with CarbonTracker XCO_2 focusing on aerosols and thin clouds, Atmos. Meas. Tech., 5, 1935–1952, doi:10.5194/amt-5-1935-2012, 2012a.

Heymann, J., Bovensmann, H., Buchwitz, M., Burrows, J. P., Deutscher, N. M., Notholt, J., Rettinger, M., Reuter, M., Schneising, O., Sussmann, R., and Warneke, T.: SCIAMACHY WFM-DOAS XCO_2: reduction of scattering related errors, Atmos. Meas. Tech., 5, 2375–2390, doi:10.5194/amt-5-2375-2012, 2012b.

Jacobson, M. Z.: Correction to "Control of fossil-fuel particulate black carbon and organic matter, possibly the most effective method of slowing global warming", J. Geophys. Res., 110, D14105, doi:10.1029/2005JD005888, 2005.

Keppel-Aleks, G., Wennberg, P. O., and Schneider, T.: Sources of variations in total column carbon dioxide, Atmos. Chem. Phys., 11, 3581–3593, doi:10.5194/acp-11-3581-2011, 2011.

Kuze, A., Suto, H., Nakajima, M., and Hamazaki, T.: Thermal and near infrared sensor for carbon observation Fourier-transform spectrometer on the Greenhouse Gases Observing Satellite for greenhouse gases monitoring, Appl. Optics, 48, 6716–6733, 2009.

Meirink, J. F., Eskes, H. J., and Goede, A. P. H.: Sensitivity analysis of methane emissions derived from SCIAMACHY observations through inverse modelling, Atmos. Chem. Phys., 6, 1275–1292, doi:10.5194/acp-6-1275-2006, 2006.

Messerschmidt, J., Geibel, M. C., Blumenstock, T., Chen, H., Deutscher, N. M., Engel, A., Feist, D. G., Gerbig, C., Gisi, M., Hase, F., Katrynski, K., Kolle, O., Lavrič, J. V., Notholt, J., Palm, M., Ramonet, M., Rettinger, M., Schmidt, M., Sussmann, R., Toon, G. C., Truong, F., Warneke, T., Wennberg, P. O., Wunch, D., and Xueref-Remy, I.: Calibration of TCCON column-averaged CO_2: the first aircraft campaign over European TCCON sites, Atmos. Chem. Phys., 11, 10765–10777, doi:10.5194/acp-11-10765-2011, 2011.

O'Dell, C. W., Connor, B., Bösch, H., O'Brien, D., Frankenberg, C., Castano, R., Christi, M., Eldering, D., Fisher, B., Gunson, M., McDuffie, J., Miller, C. E., Natraj, V., Oyafuso, F., Polonsky, I., Smyth, M., Taylor, T., Toon, G. C., Wennberg, P. O., and Wunch, D.: The ACOS CO_2 retrieval algorithm – Part 1: Description and validation against synthetic observations, Atmos. Meas. Tech., 5, 99–121, doi:10.5194/amt-5-99-2012, 2012.

Oshchepkov, S., Bril, A., Yokota, T., Morino, I., Yoshida, Y., Matsunaga, T., Belikov, D., Wunch, D., Wennberg, P., Toon, G., O'Dell, C., Butz, A., Guerlet, S., Cogan, A., Boesch, H., Eguchi, N., Deutscher, N., Griffith, D., Macatangay, R., Notholt, J., Sussmann, R., Rettinger, M., Sherlock, V., Robinson, J., Kyro, E., Heikkinen, P., Feist, D. G., Nagahama, T., Kadygrow, N., Maksyutov, S., Uchino, O., and Watanabe, H.: Effects of atmospheric light scattering on spectroscopic observations of greenhouse gases from space: validation of PPDF-based CO_2 retrievals from GOSAT, J. Geophys. Res.-Atmos., 117, 1–18, 2012.

Parker, R., Boesch, H., Cogan, A., Fraser, A., Feng, L, Palmer, P., Messerschmidt, J., Deutscher, N., Griffith, D., Notholt, J., Wennberg, P., and Wunch, D.: Methane observations from the greenhouse gases observing satellite: comparison to ground-based TCCON data and model calculations, Geophys. Res. Lett., 38, L15807, doi:10.1029/2011GL047871, 2011.

Peters, W., Jacobson, A. R., Sweeney, C., Andrews, A. E., Conway, T. J., Masarie, K., Miller, J. B., Bruhwiler, L. M. P., Pétron, G., Hirsch, A. I., Worthy, D. E. J., van der Werf, G. R., Randerson, J. T., Wennberg, P. O., Krol, M. C., and Tans, P. P.: An atmospheric perspective on North American carbon dioxide exchange: CarbonTracker, P. Natl. Acad. Sci. USA, 104, 18925–18930, doi:10.1073/pnas.0708986104, 2007.

Prather, M. J.: Lifetimes and eigenstates in atmospheric chemistry, Geophys. Res. Lett. 21, 801–804, doi:10.1029/94GL00840, 1994.

Prather, M. J., Ehhalt, D., Dentener, F., Derwent, R., Dlugokencky, E., Holland, E., Isaksen, I., Katima, J., Kirchho, V., Matson, P., Midgley, P., and Wang, M.: atmospheric chemistry and greenhouse gases, in: Climate Change 2001: The Scientific Basis, Third Assessment Report of the Intergovernmental Panel on Climate Change, edited by: Houghton, J., Ding, Y., Griggs, D., Noguer, M., van der Linden, P., Dai, X., Maskell, K., and Johnson, C., Cambridge University Press, Cambridge, UK, 2001.

Reuter, M., Buchwitz, M., Schneising, O., Heymann, J., Bovensmann, H., and Burrows, J. P.: A method for improved SCIAMACHY CO_2 retrieval in the presence of optically thin clouds, Atmos. Meas. Tech., 3, 209–232, doi:10.5194/amt-3-209-2010, 2010.

Reuter, M., Bovensmann, H., Buchwitz, M., Burrows, J. P., Connor, B. J., Deutscher, N. M., Griffith, D. W. T., Heymann, J., Keppel-Aleks, G., Messerschmidt, J., Notholt, J., Petri, C., Robinson, J., Schneising, O., Sherlock, V., Velazco, V., Warneke, T., Wennberg, P. O., and Wunch, D.: Retrieval of atmospheric CO_2 with enhanced accuracy and precision from SCIAMACHY: validation with FTS measurements and comparison with model results, J. Geophys. Res., 116, D04301, doi:10.1029/2010JD015047, 2011.

Reuter, M. and the GHG-CCI project team: ESA Climate Change Initiative (CCI) Algorithm Theoretical Basis Document Version 1 (ATBDv1) for the Essential Climate Variable (ECV) Greenhouse Gases (GHG), 15 March 2012, available at: http://www.esa-ghg-cci.org (last access: 1 October 2013), 2012.

Reuter, M., Bösch, H., Bovensmann, H., Bril, A., Buchwitz, M., Butz, A., Burrows, J. P., O'Dell, C. W., Guerlet, S., Hasekamp, O., Heymann, J., Kikuchi, N., Oshchepkov, S., Parker, R., Pfeifer, S., Schneising, O., Yokota, T., and Yoshida, Y.: A joint effort to deliver satellite retrieved atmospheric CO_2 concentrations for surface flux inversions: the ensemble median algorithm EMMA, Atmos. Chem. Phys., 13, 1771–1780, doi:10.5194/acp-13-1771-2013, 2013.

Rigby, M., Prinn, R. G., Fraser, P. J., Simmonds, P. G., Langenfelds, R. L., Huang, J., Cunnold, D. M.,Steele, L. P., Krummel, P. B., Weiss, R. F., O'Doherty, S., Salameh, P. K., Wang, H. J., Harth, C. M., Mühle, J., and Porter, L. W.: Renewed growth of atmospheric methane, Geophys. Res. Lett., 35, L22805, doi:10.1029/2008GL036037, 2008.

Rodgers, C. D.: Inverse Methods for Atmospheric Sounding: Theory and Practice, World Scientific Publishing, 2000.

Schepers, D., Guerlet, S., Butz, A., Landgraf, J., Frankenberg, C., Hasekamp, O., Blavier, J.-F., Deutscher, N. M., Griffith, D. W. T., Hase, F., Kyro, E., Morino, I., Sherlock, V., Sussmann, R., and Aben, I.: Methane retrievals from Greenhouse Gases Observing Satellite (GOSAT) shortwave infrared measurements: performance comparison of proxy and physics retrieval algorithms, J. Geophys. Res., 117, D10307, doi:10.1029/2012JD017549, 2012.

AMTD
6, 8679–8741, 2013

Schneising, O., Buchwitz, M., Burrows, J. P., Bovensmann, H., Reuter, M., Notholt, J., Macatangay, R., and Warneke, T.: Three years of greenhouse gas column-averaged dry air mole fractions retrieved from satellite – Part 1: Carbon dioxide, Atmos. Chem. Phys., 8, 3827–3853, doi:10.5194/acp-8-3827-2008, 2008.

Schneising, O., Buchwitz, M., Burrows, J. P., Bovensmann, H., Bergamaschi, P., and Peters, W.: Three years of greenhouse gas column-averaged dry air mole fractions retrieved from satellite – Part 2: Methane, Atmos. Chem. Phys., 9, 443–465, doi:10.5194/acp-9-443-2009, 2009.

Schneising, O., Buchwitz, M., Reuter, M., Heymann, J., Bovensmann, H., and Burrows, J. P.: Long-term analysis of carbon dioxide and methane column-averaged mole fractions retrieved from SCIAMACHY, Atmos. Chem. Phys., 11, 2863–2880, doi:10.5194/acp-11-2863-2011, 2011.

Schneising, O., Bergamaschi, P., Bovensmann, H., Buchwitz, M., Burrows, J. P., Deutscher, N. M., Griffith, D. W. T., Heymann, J., Macatangay, R., Messerschmidt, J., Notholt, J., Rettinger, M., Reuter, M., Sussmann, R., Velazco, V. A., Warneke, T., Wennberg, P. O., and Wunch, D.: Atmospheric greenhouse gases retrieved from SCIAMACHY: comparison to ground-based FTS measurements and model results, Atmos. Chem. Phys., 12, 1527–1540, doi:10.5194/acp-12-1527-2012, 2012.

Shapiro, S. S. and Wilk, M. B.: An analysis of variance test for normality (complete samples), Biometrika, 52, 591–611, doi:10.1093/biomet/52.3-4.591, 1965.

Simpson, I. J., Sulbaek Andersen, M. P., Meinardi, S., Bruhwiler, L., Blake, N. J., Helmig, D., Rowland, F. S., and Blake, D. R.: Long-term decline of global atmospheric ethane concentrations and implications for methane, Nature, 488, 490–494, doi:10.1038/nature11342, 2012.

Snedecor, G. W. and Cochran, W. G.: Statistical Methods, 8th Edn., Iowa State University Press, 1989.

Solomon, S., Qin, D., Manning, M., Chen, Z., Marquis, M., Averyt, K. B., Tignor, M., and Miller, H. L. (Eds.): Climate Change 2007: The Physical Science Basis, Contribution of Working Group I to the Fourth Assessment Report of the Intergovernmental Panel on Climate Change (IPCC), Cambridge University Press, Cambridge, UK and New York, NY, USA, 2007.

Stephens, B. B., Gurney, K. R., Tans, P. P., Sweeney, C., Peters, W., Bruhwiler, L., Ciais, P., Ramonet, M., Bousquet, P., Nakazawa, T., Aoki, S., Machida, T., Inoue, G., Vinnichenko, N., Lloyd, J., Jordan, A., Heimann, M., Shibistova, O., Langenfelds, R. L., Steele, L. P., Francey, R. J., and Denning, A. S.: Weak northern and strong tropical

land carbon uptake from vertical profiles of atmospheric CO_2, Science, 316, 1732–1735, doi:10.1126/science.1137004, 2007.
Washenfelder, R. A., Toon, G. C., Blavier, J.-F., Yang, Z., Allen, N. T., Wennberg, P. O., Vay, S. A., Matross, D. M., and Daube, B. C.: Carbon dioxide column abundances at the Wisconsin Tall Tower site, J. Geophys. Res., 111, D22305, doi:10.1029/2006JD007154, 2006.
Wunch, D., Toon, G. C., Wennberg, P. O., Wofsy, S. C., Stephens, B. B., Fischer, M. L., Uchino, O., Abshire, J. B., Bernath, P., Biraud, S. C., Blavier, J.-F. L., Boone, C., Bowman, K. P., Browell, E. V., Campos, T., Connor, B. J., Daube, B. C., Deutscher, N. M., Diao, M., Elkins, J. W., Gerbig, C., Gottlieb, E., Griffith, D. W. T., Hurst, D. F., Jiménez, R., Keppel-Aleks, G., Kort, E. A., Macatangay, R., Machida, T., Matsueda, H., Moore, F., Morino, I., Park, S., Robinson, J., Roehl, C. M., Sawa, Y., Sherlock, V., Sweeney, C., Tanaka, T., and Zondlo, M. A.: Calibration of the Total Carbon Column Observing Network using aircraft profile data, Atmos. Meas. Tech., 3, 1351–1362, doi:10.5194/amt-3-1351-2010, 2010.
Wunch, D., Toon, G. C., Blavier, J.-F. L., Washenfelder, R. A., Notholt, J., Connor, B. J., Griffith, D. W. T., Sherlock, V., and Wennberg, P. O.: The Total Carbon Column Observing Network, Philos. T. Roy. Soc. A, 369, 2087–2112, doi:10.1098/rsta.2010.0240, 2011a.
Wunch, D., Wennberg, P. O., Toon, G. C., Connor, B. J., Fisher, B., Osterman, G. B., Frankenberg, C., Mandrake, L., O'Dell, C., Ahonen, P., Biraud, S. C., Castano, R., Cressie, N., Crisp, D., Deutscher, N. M., Eldering, A., Fisher, M. L., Griffith, D. W. T., Gunson, M., Heikkinen, P., Keppel-Aleks, G., Kyrö, E., Lindenmaier, R., Macatangay, R., Mendonca, J., Messerschmidt, J., Miller, C. E., Morino, I., Notholt, J., Oyafuso, F. A., Rettinger, M., Robinson, J., Roehl, C. M., Salawitch, R. J., Sherlock, V., Strong, K., Sussmann, R., Tanaka, T., Thompson, D. R., Uchino, O., Warneke, T., and Wofsy, S. C.: A method for evaluating bias in global measurements of CO_2 total columns from space, Atmos. Chem. Phys., 11, 12317–12337, doi:10.5194/acp-11-12317-2011, 2011b.

Table 1. List of all GHG-CCI algorithms, inter-compared in this study, their time coverage, and references. *OCFC and SRFC are bias corrected versions of OCFP and SRFP, respectively.

Molec	Algorithm	Institute	Satellite	Time covered	References
XCO_2	BESD v01.00.01	IUP	SCIAMACHY	Jan 2006–Dec 2011	Reuter et al. (2010, 2011)
XCO_2	WFMD v2.2	IUP	SCIAMACHY	Jan 2003–Dec 2009	Schneising et al. (2011, 2012), Heymann et al. (2012b)
XCO_2	OCFC* v3.0	UoL	GOSAT	Apr 2009–May 2011	Cogan et al. (2012)
XCO_2	SRFC* v1.1	SRON	GOSAT	Apr 2009–Apr 2011	Butz et al. (2011)
XCH_4	IMAP v6.0	SRON	SCIAMACHY	Jan 2003–Dec 2010	Frankenberg et al. (2011)
XCH_4	WFMD v2.3	IUP	SCIAMACHY	Jan 2003–Dec 2009	Schneising et al. (2010, 2011)
XCH_4	OCFP v3.2	UoL	GOSAT	Apr 2009–Apr 2011	Parker et al. (2011)
XCH_4	OCPR v3.2	UoL	GOSAT	Apr 2009–Apr 2011	Parker et al. (2011)
XCH_4	SRFP v1.1	SRON	GOSAT	Apr 2009–May 2011	Butz et al. (2011)
XCH_4	SRPR v1.1	SRON	GOSAT	Apr 2009–May 2011	Schepers et al. (2012)

AMTD
6, 8679–8741, 2013

Table 2. List of all participating TCCON stations, their location, time coverage and number of data (N).

TCCON station name	Lat (°)	Lon (°)	Alt (m)	Time	N
Bialystok (BIA)	53.23	23.03	183	Mar 2009–Nov 2011	31 256
Bremen (BRE)	53.10	8.85	7	Jan 2007–Nov 2011	10 634
Karlsruhe (KAR)	49.10	8.44	110	Apr 2010–Nov 2011	8586
Orleans (ORL)	47.96	2.11	132	Aug 2009–Nov 2011	18 169
Garmisch (GAR)	47.48	11.06	744	May 2009–Nov 2011	26 528
Park Falls (PAR)	45.94	−90.27	442	Jun 2004–Aug 2012	169 912
Lamont (LAM)	36.60	−97.49	320	Jul 2008–Aug 2012	207 855
Darwin (DAR)	−12.42	130.89	30	Aug 2005–Nov 2011	158 879
Wollongong (WOL)	−34.41	150.88	30	Jun 2008–Nov 2011	40 622
Lauder (LAU)	−45.05	169.68	370	Jun 2004–Nov 2011	117 349

AMTD
6, 8679–8741, 2013

Table 3. BESD and WFMD XCO_2 validation results for all individual stations and using all data combined (ALL, in bold). All results apart from R and N are in ppm units. The Relative Accuracy (RA, in bold) is the standard deviation over all the above listed individual station results. * This station has been excluded from the relative accuracy calculation flagged by *.

	BESD/SCIA XCO_2				WFMD/SCIA XCO_2			
station	Bias	Scatter	R	N	Bias	Scatter	R	N
BIA	0.12	1.99	0.85	504	0.03	5.04	0.56	1714
BRE	−0.20	2.53	0.75	237	0.34	5.14	0.50	1354
ORL	0.53	2.40	0.22	166	2.17	4.07	0.19	209
GAR	1.43	2.10	0.80	144	0.22	6.34	0.11	551
PAR	0.45	2.67	0.83	738	−1.35	5.27	0.70	8206
LAM	−0.78	2.08	0.78	2338	−1.58	4.13	0.46	11 288
DAR	0.24	2.66	0.76	4890	−2.13	4.16	0.41	7250
WOL	0.26	2.64	0.67	654	−0.44	4.67	0.27	1061
LAU*	3.66	1.21	–	3	0.19	6.41	0.04	185
ALL	**0.02**	**2.53**	**0.81**	**9674**	**−1.37**	**4.69**	**0.61**	**31 818**
RA	**1.28**				**1.29**			
	0.63*				**1.36***			

AMTD
6, 8679–8741, 2013

The Greenhouse Gas Climate Change Initiative (GHG-CCI)

B. Dils et al.

Table 4. BESD and WFMD XCO_2 seasonal mean bias results for individual stations and all data combined (ALL, in bold). Values that did not meet the quality requirements are not listed. The seasonality (Seas, in bold), corresponds with the standard deviation over the 4 seasonal bias values per station. The Seasonal Relative Accuracy (SRA, in bold) corresponds with the standard deviation over all (common) seasonal bias values over all individual stations. All results are in ppm units.

	BESD/SCIA XCO_2					WFMD/SCIA XCO_2				
station	JFM	AMJ	JAS	OND	Seas	JFM	AMJ	JAS	OND	Seas
BIA	–	0.07	0.69	–	**–**	–	0.01	0.09	–	**–**
BRE	–	−0.19	0.34	–	**–**	–	0.17	0.76	–	**–**
ORL	–	–	0.68	−1.70	**–**	–	–	2.15	–	**–**
GAR	–	1.98	1.31	–	**–**	–	−1.72	1.09	–	**–**
PAR	–	0.33	1.04	−1.52	**–**	–	−1.48	−1.27	−1.62	**–**
LAM	0.13	−0.69	−1.07	−0.69	**0.51**	−2.52	−3.08	−0.88	−0.92	**1.12**
DAR	−0.96	0.48	0.59	−0.71	**0.80**	−1.28	−2.62	−2.80	0.67	**1.60**
WOL	3.83	–	−0.62	0.07	**–**	−0.25	–	1.03	−1.42	**–**
LAU	–	–	–	–	**–**	–	–	–	–	**–**
ALL	**−0.34**	**0.20**	**0.20**	**−0.57**	**0.39**	**−1.88**	**−1.79**	**−1.21**	**−0.66**	**0.57**
SRA	**1.19**					**1.43**				

AMTD
6, 8679–8741, 2013

The Greenhouse Gas Climate Change Initiative (GHG-CCI)

B. Dils et al.

Table 5. OCFC and SRFC XCO_2 validation results for all individual stations and using all data combined (ALL, in bold). All results apart from R and N are in ppm units. The Relative Accuracy (RA, in bold) is the standard deviation over all the above listed individual station results. * This station has been excluded from the relative accuracy calculation flagged by *.

	OCFC/GOSAT XCO_2				SRFC/GOSAT XCO_2			
station	Bias	Scatter	R	N	Bias	Scatter	R	N
BIA	−0.52	2.73	0.87	157	−0.13	2.76	0.82	174
BRE	−0.50	2.80	0.68	92	−0.90	2.40	0.83	81
KAR	−0.61	2.87	0.72	188	−1.08	2.51	0.83	151
ORL	−0.72	2.81	0.80	247	−0.83	2.39	0.90	223
GAR	0.31	2.72	0.78	182	0.32	2.66	0.82	168
PAR	−1.31	1.91	0.92	211	−0.77	2.52	0.91	268
LAM	−1.04	1.99	0.78	1432	−0.84	2.14	0.83	1274
DAR	−0.96	2.07	0.33	117	0.67	2.56	0.21	81
WOL	0.15	2.66	0.41	239	0.88	3.27	0.33	189
LAU*	0.71	2.98	0.63	25	−1.74	3.90	0.15	24
ALL	**−0.76**	**2.37**	**0.79**	**2890**	**−0.57**	**2.50**	**0.81**	**2633**
RA	**0.64**				**0.84**			
	0.53*				**0.75***			

AMTD
6, 8679–8741, 2013

Table 6. OCFC and SRFC XCO_2 seasonal mean bias results for individual stations and all data combined (ALL, in bold). Values that did not meet the quality requirements are not listed. The seasonality (Seas, in bold), corresponds with the standard deviation over the 4 seasonal bias values per station. The Seasonal Relative Accuracy (SRA, in bold) corresponds with the standard deviation over all (common) seasonal bias values over all individual stations. All results are in ppm units.

	OCFC/GOSAT XCO_2					SRFC/GOSAT XCO_2				
station	JFM	AMJ	JAS	OND	Seas	JFM	AMJ	JAS	OND	Seas
BIA	–	0.26	−0.68	–	–	–	−0.20	0.37	–	–
BRE	−1.77	0.76	−0.99	–	–	–	−0.26	−1.79	–	–
KAR	−2.02	0.21	−0.20	–	–	−1.90	−0.70	−0.83	–	–
ORL	−3.30	0.73	−0.52	–	–	−2.09	−0.37	−0.41	−1.31	**0.82**
GAR	0.08	–	0.96	−2.08	–	–	–	0.54	–	–
PAR	–	−0.55	−2.04	−1.40	–	0.23	0.15	−1.34	−0.74	**0.75**
LAM	−1.42	0.09	−0.81	−1.64	**0.78**	−1.03	−0.69	−0.68	−0.99	**0.19**
DAR	–	−1.04	−0.85	–	–	–	–	1.39	–	–
WOL	1.52	−0.04	−0.45	–	–	–	–	0.73	–	–
LAU	–	–	–	–	–	–	–	–	–	–
ALL	**−1.15**	**0.15**	**−0.58**	**−1.56**	**0.74**	**−0.85**	**−0.35**	**−0.33**	**−0.97**	**0.33**
SRA	**1.08**					**0.89**				

Discussion Paper | Discussion Paper | Discussion Paper | Discussion Paper |

AMTD
6, 8679–8741, 2013

The Greenhouse Gas Climate Change Initiative (GHG-CCI)

B. Dils et al.

Title Page
Abstract Introduction
Conclusions References
Tables Figures
Back Close
Full Screen / Esc
Printer-friendly Version
Interactive Discussion

Table 7. IMAP and WFMD XCH_4 validation results for all individual stations and using all data combined (ALL, in bold). All results apart from R and N are in ppb units. The Relative Accuracy (RA, in bold) is the standard deviation over all the above listed individual station results.

	IMAP/SCIA XCH_4				WFMD/SCIA XCH_4			
station	Bias	Scatter	R	N	Bias	Scatter	R	N
BIA	14.2	42.1	0.29	1228	2.7	85.5	−0.13	2067
BRE	−1.2	54.1	0.17	946	−5.9	88.6	0.21	1516
ORL	0.2	47.9	0.26	287	−6.0	74.7	0.16	255
GAR	10.7	49.8	0.34	641	−4.7	92.6	0.34	630
PAR	2.3	48.9	0.30	22 078	3.7	75.1	0.09	13 607
LAM	11.8	46.0	0.25	9430	2.1	74.0	−0.01	10 808
DAR	−25.3	51.9	0.16	6500	−13.5	72.6	0.10	8044
WOL	−24.0	46.2	−0.23	881	−19.3	79.4	−0.10	1377
LAU	−10.6	49.6	0.23	329	−9.8	91.1	0.01	287
ALL	**−0.1**	**50.2**	**0.65**	**42 320**	**−1.9**	**76.4**	**0.44**	**38 591**
RA	**14.7**				**7.8**			

AMTD
6, 8679–8741, 2013
The Greenhouse Gas Climate Change Initiative (GHG-CCI)
B. Dils et al.

Table 8. IMAP and WFMD XCH_4 seasonal mean bias results for individual stations and all data combined (ALL, in bold). Values that did not meet the quality requirements are not listed. The seasonality (Seas, in bold), corresponds with the standard deviation over the 4 seasonal bias values per station. The Seasonal Relative Accuracy (SRA, in bold) corresponds with the standard deviation over all (common) seasonal bias values over all individual stations. All results are in ppb units.

	IMAP/SCIA XCH_4					WFMD/SCIA XCH_4				
station	JFM	AMJ	JAS	OND	Seas	JFM	AMJ	JAS	OND	Seas
BIA	–	13.9	14.4	–	–	–	5.7	−4.2	–	–
BRE	35.9	1.9	−7.9	−5.4	**20.3**	–	−10.6	3.1	–	–
ORL	–	–	7.4	−1.6	–	–	–	−7.1	–	–
GAR	–	1.8	10.7	22.8	–	–	−20.9	5.0	–	–
PAR	14.3	6.9	3.9	−7.3	**9.0**	7.1	7.8	1.4	−1.6	**4.5**
LAM	–	18.2	18.4	3.0	–	−8.7	6.1	15.9	−15.2	**14.1**
DAR	−10.6	−37.7	−23.4	−9.4	**13.2**	1.8	−18.3	−14.6	−10.8	**8.7**
WOL	–	–	−41.7	−18.6	–	−45.8	–	−3.1	−22.1	–
LAU	–	–	–	−13.3	–	−10.1	–	–	−0.0	–
ALL	**5.1**	**−0.1**	**2.5**	**−4.4**	**4.0**	**−7.3**	**0.5**	**1.3**	**−12.5**	**6.6**
SRA	**17.2**					**10.5**				

AMTD
6, 8679–8741, 2013

The Greenhouse Gas Climate Change Initiative (GHG-CCI)

B. Dils et al.

Table 9. OCPR and OCFP XCH_4 validation results for all individual stations and using all data combined (ALL, in bold). All results apart from R and N are in ppb units. The Relative Accuracy (RA, in bold) is the standard deviation over all the above listed individual station results.

	OCPR/GOSAT XCH_4				OCFP/GOSAT XCH_4			
station	Bias	Scatter	R	N	Bias	Scatter	R	N
BIA	8.3	13.8	0.54	799	3.4	18.6	0.31	213
BRE	5.4	12.6	0.54	279	2.9	14.6	0.25	128
KAR	4.8	13.7	0.52	576	−2.0	17.7	0.14	267
ORL	6.6	12.9	0.49	597	1.0	15.8	0.22	286
GAR	12.1	14.1	0.39	623	8.0	18.1	0.13	232
PAR	5.9	14.0	0.50	887	4.2	16.6	0.51	263
LAM	8.0	14.8	0.49	2757	−0.5	18.1	0.47	1603
DAR	5.8	10.1	0.47	312	−13.9	13.3	0.28	68
WOL	2.4	12.9	0.69	636	−2.9	20.8	0.38	225
LAU	3.6	8.6	0.83	203	−4.7	16.6	0.48	35
ALL	**7.0**	**14.0**	**0.87**	**7669**	**0.4**	**18.1**	**0.78**	**3320**
RA	**2.7**				**6.0**			

Discussion Paper | Discussion Paper | Discussion Paper | Discussion Paper |

AMTD

6, 8679–8741, 2013

The Greenhouse Gas Climate Change Initiative (GHG-CCI)

B. Dils et al.

Title Page
Abstract Introduction
Conclusions References
Tables Figures
Back Close
Full Screen / Esc
Printer-friendly Version
Interactive Discussion

Table 10. SRPR and SRFP XCH_4 validation results for all individual stations and using all data combined (ALL, in bold). All results apart from R and N are in ppb units. The Relative Accuracy (RA, in bold) is the standard deviation over all the above listed individual station results.

	SRPR/GOSAT XCH_4				SRFP/GOSAT XCH_4			
station	Bias	Scatter	R	N	Bias	Scatter	R	N
BIA	9.5	14.7	0.53	423	−0.4	14.2	0.60	174
BRE	2.4	15.7	0.38	125	−4.3	14.9	0.26	81
KAR	1.5	16.9	0.39	322	−5.6	13.3	0.54	151
ORL	6.8	14.2	0.37	359	−2.6	13.4	0.18	223
GAR	7.7	19.4	0.30	345	2.4	16.3	0.28	168
PAR	0.5	15.0	0.44	679	−2.5	14.8	0.50	268
LAM	2.7	13.0	0.74	2096	−2.8	13.9	0.60	1274
DAR	−3.8	8.3	0.66	157	−3.4	14.8	0.14	81
WOL	−1.0	13.4	0.56	418	−2.1	21.4	0.27	189
LAU	5.9	11.7	0.85	82	−8.7	16.2	0.58	24
ALL	**3.1**	**14.6**	**0.87**	**5006**	**−2.5**	**14.9**	**0.83**	**2633**
RA	**4.2**				**3.0**			

AMTD
6, 8679–8741, 2013

Table 11. OCPR and OCFP XCH_4 seasonal mean bias results for individual stations and all data combined (ALL, in bold). Values that did not meet the quality requirements are not listed. The seasonality (Seas, in bold), corresponds with the standard deviation over the 4 seasonal bias values per station. The Seasonal Relative Accuracy (SRA, in bold) corresponds with the standard deviation over all (common) seasonal bias values over all individual stations. All results are in ppb units.

	OCPR/GOSAT XCH_4					OCFP/GOSAT XCH_4				
station	JFM	AMJ	JJA	SON	Seas	JFM	AMJ	JJA	SON	Seas
BIA	4.5	10.4	15.1	0.4	**6.5**	−3.3	3.3	10.0	–	–
BRE	2.3	8.5	3.8	1.9	**3.0**	5.7	2.4	2.3	–	–
KAR	3.0	10.3	−0.2	−0.4	**5.0**	−2.8	−3.1	−1.3	7.2	**4.9**
ORL	1.7	12.0	8.5	0.0	**5.7**	−2.1	1.2	2.4	−1.0	**2.0**
GAR	13.5	15.4	11.9	4.6	**4.7**	8.1	5.2	11.1	0.2	**4.6**
PAR	10.1	10.7	3.7	1.7	**4.5**	4.9	5.4	4.3	3.4	**0.9**
LAM	1.5	13.9	13.4	2.6	**6.7**	−7.1	1.4	4.2	−1.8	**4.8**
DAR	15.3	−1.9	4.7	10.8	**7.5**	–	−18.7	−11.8	−13.7	–
WOL	3.2	5.3	3.3	−2.3	**3.3**	−5.5	4.4	−3.9	−2.1	**4.3**
LAU	7.2	4.3	1.0	1.9	**2.8**	−2.6	–	–	−6.1	–
ALL	**4.8**	**11.0**	**8.8**	**2.4**	**3.9**	**−2.9**	**1.3**	**3.1**	**−1.1**	**2.6**
SRA	**5.4**					**6.2**				

Discussion Paper | Discussion Paper | Discussion Paper | Discussion Paper |

AMTD

6, 8679–8741, 2013

The Greenhouse Gas Climate Change Initiative (GHG-CCI)

B. Dils et al.

Table 12. SRPR and SRFP XCH_4 seasonal mean bias results for individual stations and all data combined (ALL, in bold). Values that did not meet the quality requirements are not listed. The seasonality (Seas, in bold), corresponds with the standard deviation over the 4 seasonal bias values per station. The Seasonal Relative Accuracy (SRA, in bold) corresponds with the standard deviation over all (common) seasonal bias values over all individual stations. All results are in ppb units.

	SRPR/GOSAT XCH_4					SRFP/GOSAT XCH_4				
SRPR	JFM	AMJ	JJA	SON	Seas	JFM	AMJ	JJA	SON	Seas
BIA	5.1	10.7	10.8	−0.6	**5.4**	–	−1.8	3.2	−7.0	–
BRE	7.8	9.3	−5.1	−4.3	**7.7**	–	−3.1	−4.3	–	–
KAR	1.9	8.3	−6.1	0.5	**5.9**	−5.1	−1.7	−7.7	−7.8	**2.9**
ORL	6.6	12.9	5.0	−2.9	**6.5**	1.1	−0.5	−4.3	−10.8	**5.3**
GAR	11.0	11.7	5.5	4.3	**3.8**	7.9	4.1	1.2	0.5	**3.4**
PAR	14.6	6.9	−4.2	2.7	**7.9**	10.2	2.1	−8.1	−0.1	**7.5**
LAM	0.5	5.0	1.6	3.2	**2.0**	−4.5	−0.3	−1.5	−4.6	**2.2**
DAR	–	−7.1	−2.7	−1.4	–	–	−8.8	1.6	–	–
WOL	−6.9	3.7	1.7	−4.8	**5.1**	−6.2	7.8	−4.2	0.2	**6.2**
LAU	3.3	3.8	7.9	7.3	**2.3**	–	–	–	−16.7	–
ALL	**2.7**	**7.0**	**1.3**	**2.1**	**2.6**	**−2.0**	**−0.5**	**−2.6**	**−4.5**	**1.6**
SRA	**6.2**					**5.7**				

AMTD
6, 8679–8741, 2013

The Greenhouse Gas Climate Change Initiative (GHG-CCI)

B. Dils et al.

Table 13. Overview table, listing all overall (ALL) results. The listed uncertainties on the bias and scatter correspond with the 0.95 confidence interval. XCO_2 bias and scatter in ppm, XCH_4 bias and scatter in ppb.

algo	Bias	Scat	R	N
		SCIA/XCO_2		
BESD	0.02 ± 0.05	2.53 ± 0.04	0.81	9674
WFMD	-1.37 ± 0.05	4.69 ± 0.04	0.61	31 818
		GOSAT/XCO_2		
OCFC	-0.76 ± 0.09	2.37 ± 0.06	0.79	2890
SRFC	-0.57 ± 0.10	2.50 ± 0.07	0.81	2633
		SCIA/XCH_4		
IMAP	-0.1 ± 0.5	50.2 ± 0.3	0.65	42 320
WFMD	-1.9 ± 0.8	76.4 ± 0.5	0.44	38 591
		GOSAT/XCH_4		
OCFP	0.4 ± 0.6	18.1 ± 0.4	0.78	3320
OCPR	7.0 ± 0.3	14.0 ± 0.2	0.87	7669
SRFP	-2.5 ± 0.6	14.9 ± 0.4	0.83	2633
SRPR	3.1 ± 0.4	14.6 ± 0.3	0.87	5006

AMTD
6, 8679–8741, 2013

Table 14. Overview table, listing the "relative accuracy" (RA), overall "seasonality" (Seas) and "seasonal relative accuracy" (SRA), together with their 95 % confidence interval (RA 95 %, Seas 95 % and SRA 95 %) and the probability that the obtained sample variances stem from the same population ($P(H_0\colon \sigma_1^2 = \sigma_2^2)$). The P values for the GOSAT/$X\mathrm{CH_4}$ results correspond with the following pairs: (a) OCFP vs. OCPR, (b) OCPR vs. SRFP and (c) SRFP vs. SRPR.

Algorithm	RA	RA 95 %	P (RA)	Seas	Seas 95 %	P (Seas)	SRA	SRA 95 %	P (SRA)
				SCIA/$X\mathrm{CO_2}$					
BESD	0.63	0.42–1.28	0.06	0.39	0.22–1.45	0.55	1.19	0.91–1.72	0.42
WFMD	1.36	0.90–2.77		0.57	0.32–2.13		1.43	1.09–2.07	
				GOSAT/$X\mathrm{CO_2}$					
OCFC	0.53	0.36–0.97	0.32	0.74	0.42–2.76	0.22	1.08	0.82–1.58	0.68
SRFC	0.75	0.52–1.37		0.33	0.19–1.23		0.89	0.68–1.30	
				SCIA/$X\mathrm{CH_4}$					
IMAP	14.7	9.9–28.2	0.09	4.0	2.3–14.9	0.43	17.2	13.2–24.8	0.28
WFMD	7.8	5.3–14.9		6.6	3.7–24.6		10.5	8.0–15.2	
				GOSAT/$X\mathrm{CH_4}$					
OCFP	6.0	4.1–11.0	0.03[a]	2.6	1.5–9.7	0.52[a]	6.2	5.0–8.3	0.45[a]
OCPR	2.7	1.9–4.9	0.76[b]	3.9	2.2–14.5	0.18[b]	5.4	4.3–7.2	0.77[b]
SRFP	3.0	2.1–5.5	0.33[c]	1.6	0.9–6.0	0.45[c]	5.7	4.6–7.6	0.65[c]
SRPR	4.2	2.9–7.7		2.6	1.5–9.7		6.2	5.0–8.3	

AMTD
6, 8679–8741, 2013

The Greenhouse Gas Climate Change Initiative (GHG-CCI)

B. Dils et al.

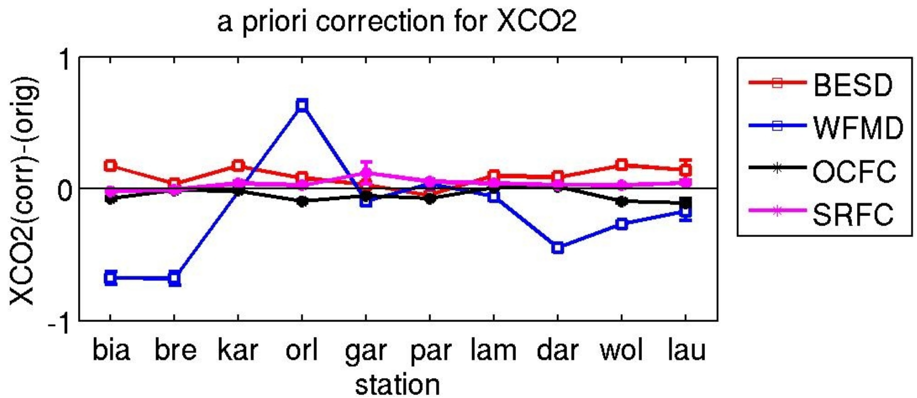

Fig. 1. Mean a priori correction (XCO_2 corrected – XCO_2 original), in ppm, on the XCO_2 result, per station.

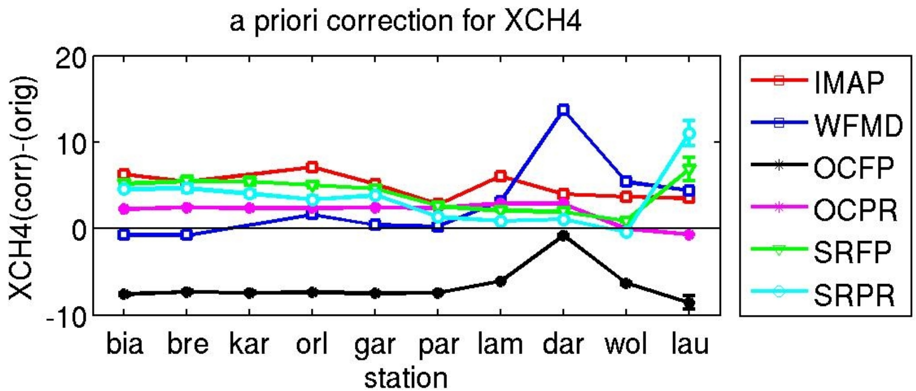

Fig. 2. Mean a priori correction (XCH_4 corrected – XCH_4 original), in ppb, on the XCH_4 result, per station.

AMTD
6, 8679–8741, 2013

The Greenhouse Gas Climate Change Initiative (GHG-CCI)

B. Dils et al.

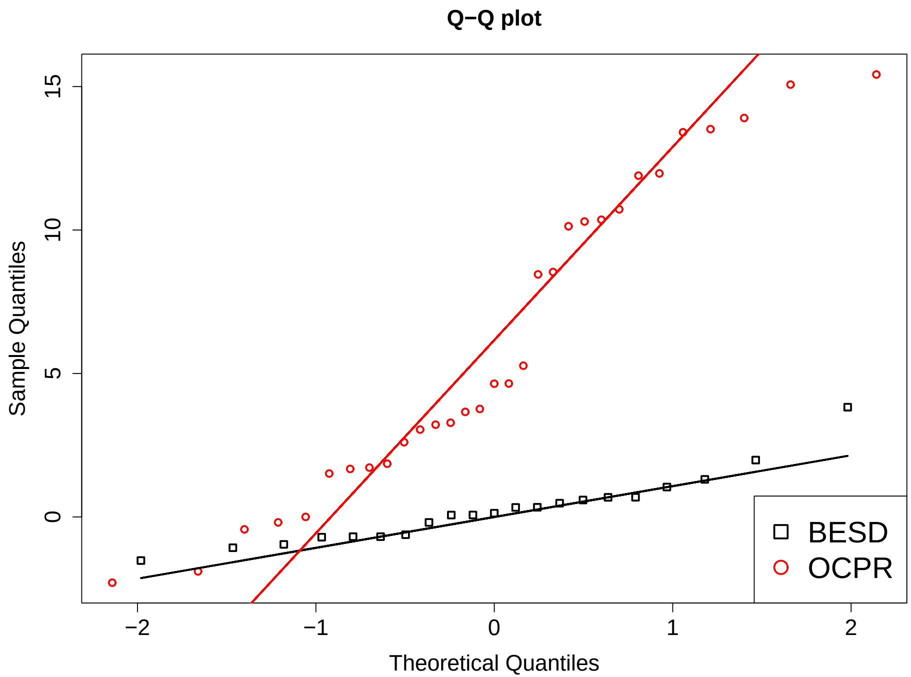

Fig. 3. Quantile–Quantile (Q–Q) plot for the BESD and OCPR SRA samples.

AMTD
6, 8679–8741, 2013

The Greenhouse Gas Climate Change Initiative (GHG-CCI)

B. Dils et al.

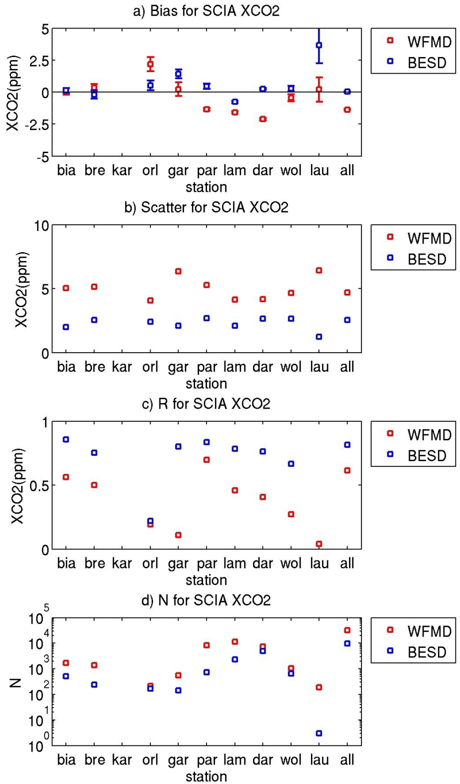

Fig. 4. SCIAMACHY XCO_2 Bias **(a)**, Scatter **(b)**, Correlation **(c)** and number of data pairs **(d)**, for all individual TCCON stations and all data combined.

AMTD
6, 8679–8741, 2013

The Greenhouse Gas Climate Change Initiative (GHG-CCI)

B. Dils et al.

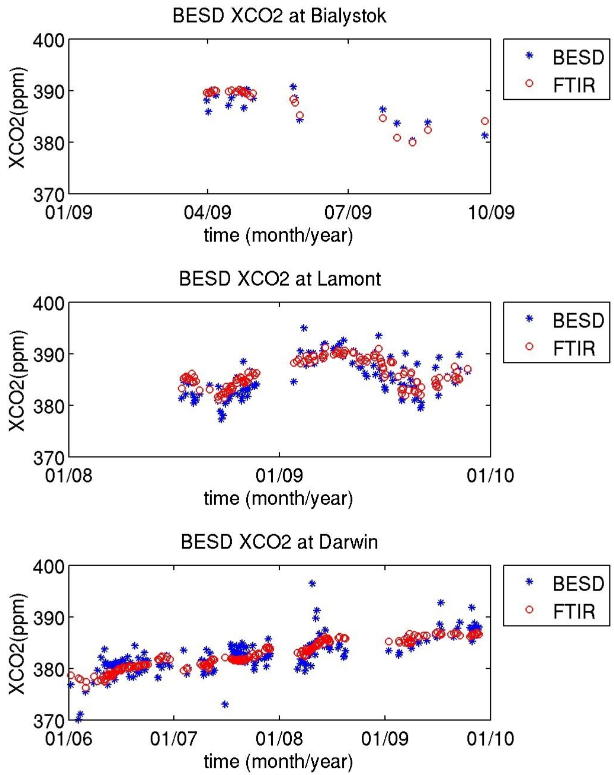

Fig. 5. Daily averaged timeseries of paired BESD and TCCON FTIR XCO_2 at Bialystok (top), Lamont (mid) and Darwin (bottom).

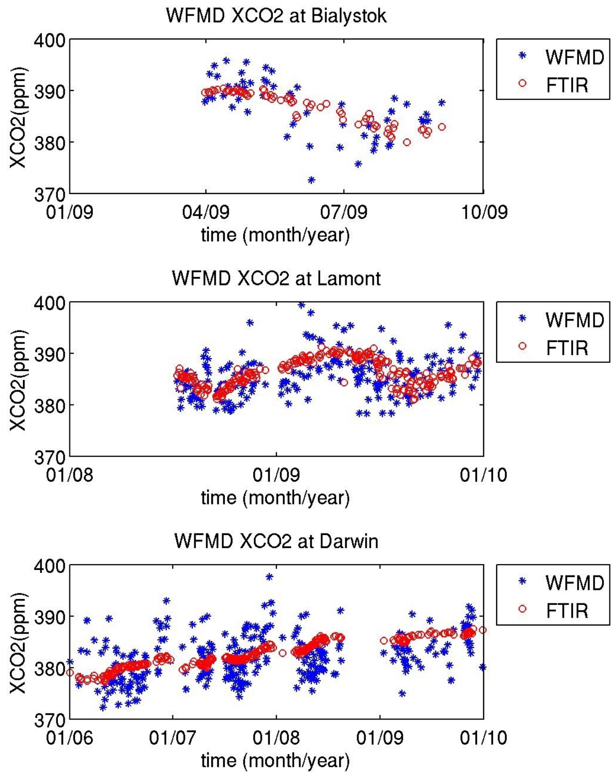

Fig. 6. Daily averaged timeseries of paired WFMD and TCCON FTIR XCO_2 at Bialystok (top), Lamont (mid) and Darwin (bottom).

AMTD
6, 8679–8741, 2013

The Greenhouse Gas Climate Change Initiative (GHG-CCI)

B. Dils et al.

Title Page
Abstract Introduction
Conclusions References
Tables Figures
◀I ▶I
◀ ▶
Back Close
Full Screen / Esc
Printer-friendly Version
Interactive Discussion

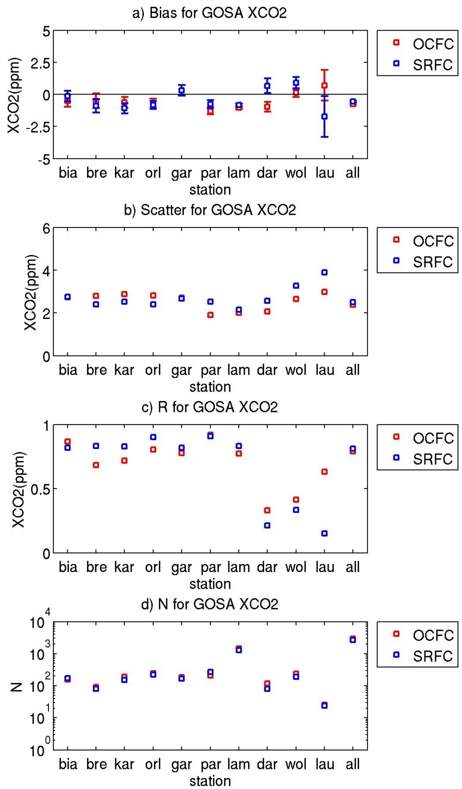

Fig. 7. GOSAT XCO_2 Bias **(a)**, Scatter **(b)**, Correlation **(c)** and number of data pairs **(d)**, for all individual TCCON stations and all data combined.

AMTD
6, 8679–8741, 2013

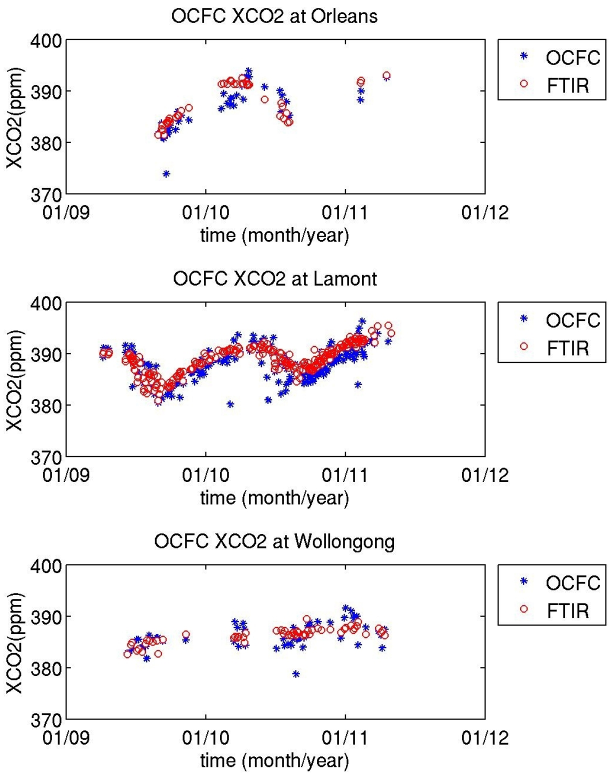

Fig. 8. Daily averaged timeseries of paired OCFC and TCCON FTIR XCO_2 at Orleans (top), Lamont (mid) and Wollongong (bottom).

AMTD
6, 8679–8741, 2013

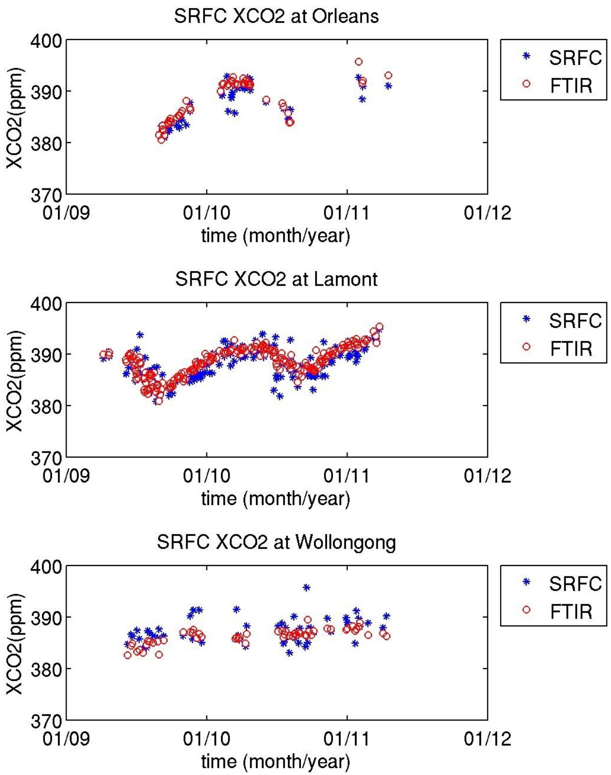

Fig. 9. Daily averaged timeseries of paired SRFC and TCCON FTIR XCO_2 at Orleans (top), Lamont (mid) and Wollongong (bottom).

AMTD
6, 8679–8741, 2013

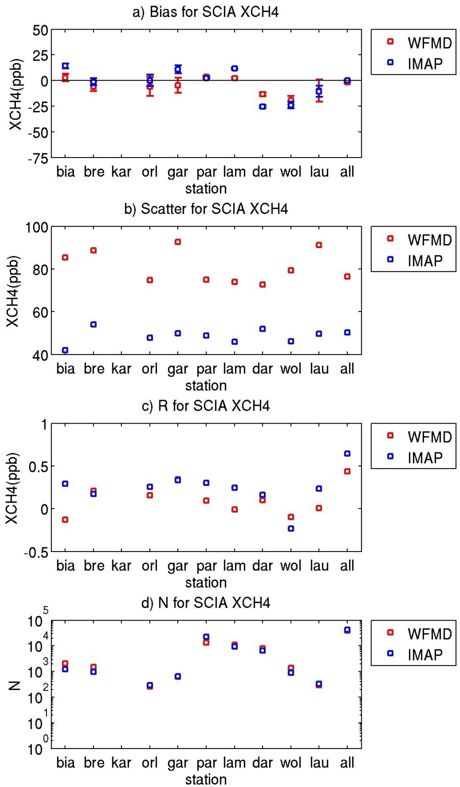

Fig. 10. SCIAMACHY XCH_4 Bias **(a)**, Scatter **(b)**, Correlation **(c)** and number of data pairs **(d)**, for all individual TCCON stations and all data combined.

AMTD
6, 8679–8741, 2013

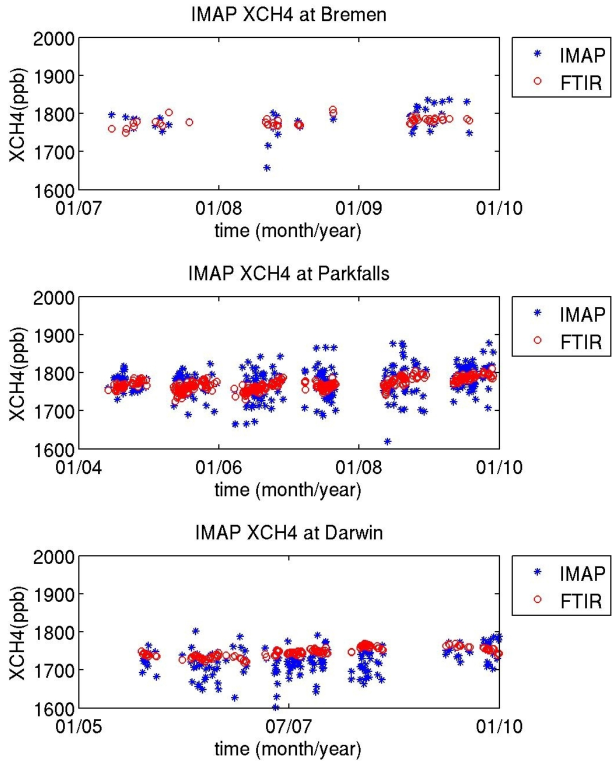

Fig. 11. Daily averaged timeseries of paired IMAP and TCCON FTIR XCH_4 at Bremen (top), Park Falls (mid) and Darwin (bottom).

AMTD
6, 8679–8741, 2013

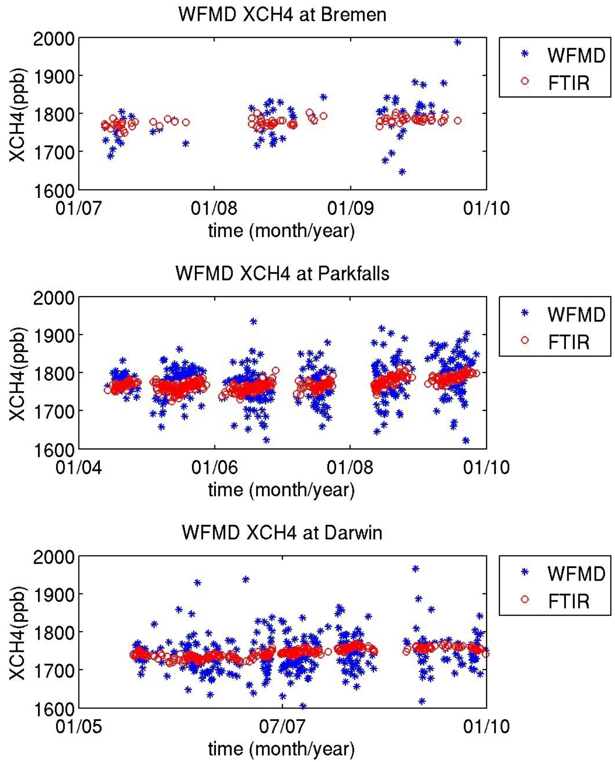

Fig. 12. Daily averaged timeseries of paired WFMD and TCCON FTIR XCH_4 at Bremen (top), Park Falls (mid) and Darwin (bottom).

AMTD
6, 8679–8741, 2013

The Greenhouse Gas Climate Change Initiative (GHG-CCI)

B. Dils et al.

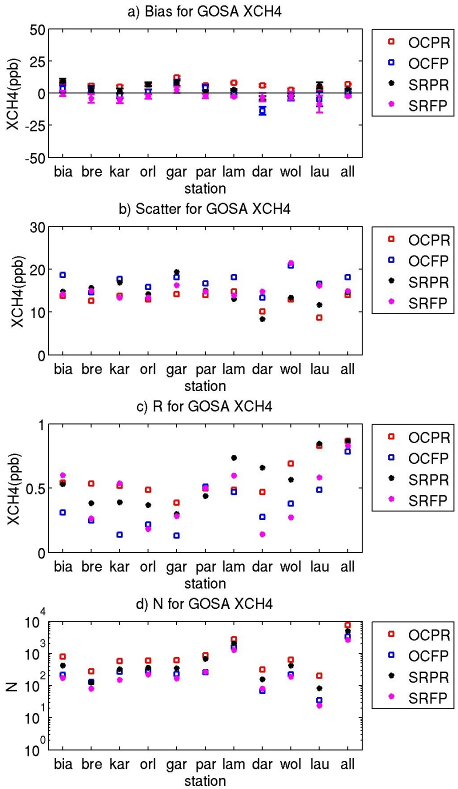

Fig. 13. GOSAT XCH_4 Bias **(a)**, Scatter **(b)**, Correlation **(c)** and number of data pairs **(d)**, for all individual TCCON stations and all data combined.

AMTD
6, 8679–8741, 2013

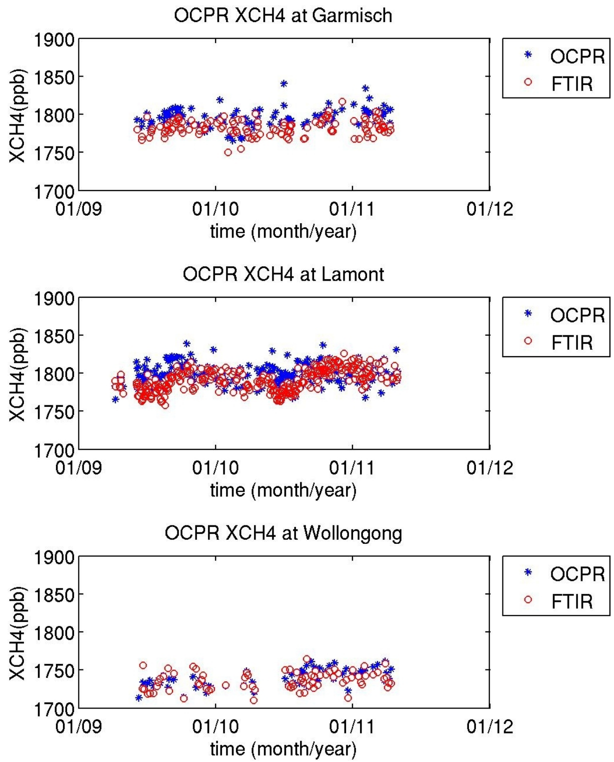

Fig. 14. Daily averaged timeseries of paired OCPR and TCCON FTIR XCH_4 at Garmisch (top), Lamont (mid) and Wollongong (bottom).

AMTD
6, 8679–8741, 2013

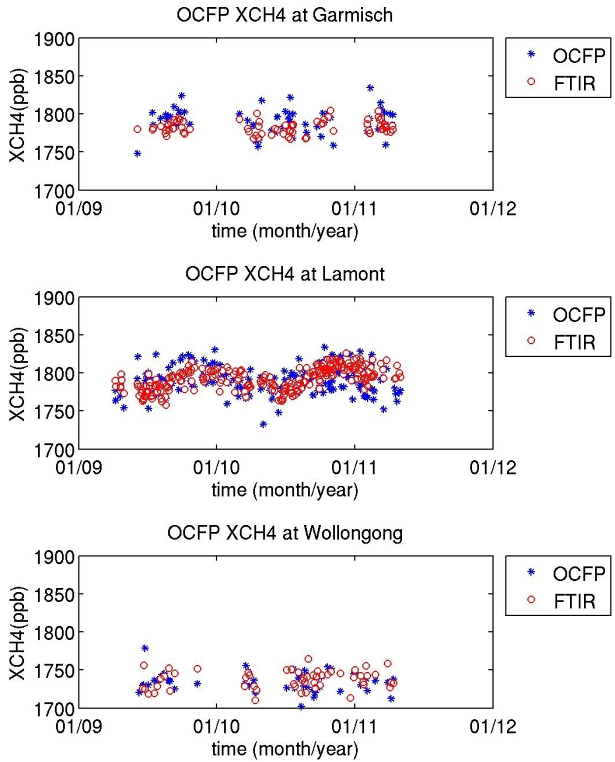

Fig. 15. Daily averaged timeseries of paired OCFP and TCCON FTIR XCH_4 at Garmisch (top), Lamont (mid) and Wollongong (bottom).

AMTD
6, 8679–8741, 2013
The Greenhouse Gas Climate Change Initiative (GHG-CCI)
B. Dils et al.

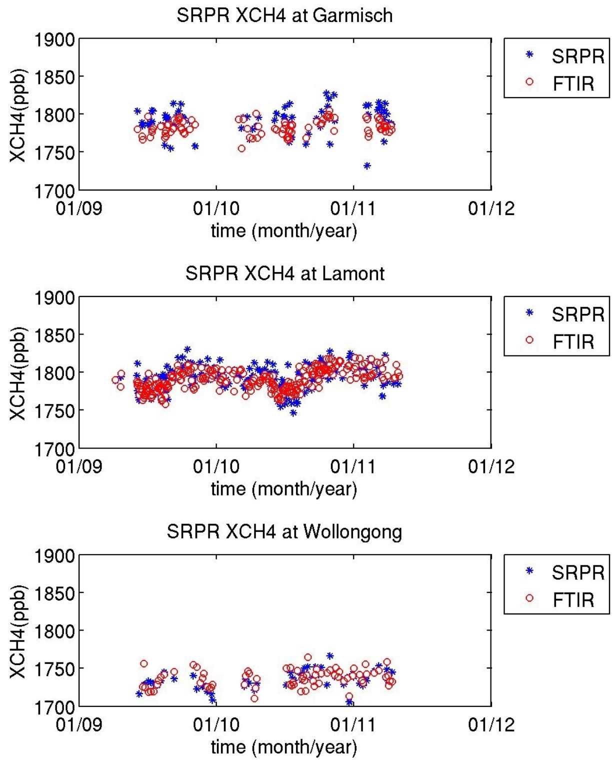

Fig. 16. Daily averaged timeseries of paired SRPR and TCCON FTIR XCH_4 at Garmisch (top), Lamont (mid) and Wollongong (bottom).

AMTD
6, 8679–8741, 2013

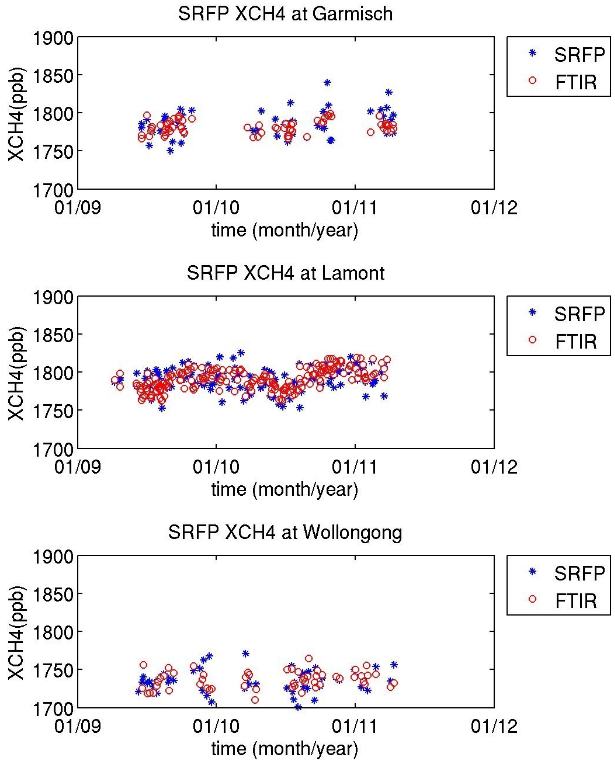

Fig. 17. Daily averaged timeseries of paired SRFP and TCCON FTIR XCH_4 at Garmisch (top), Lamont (mid) and Wollongong (bottom).

AMTD
6, 8679–8741, 2013

The Greenhouse Gas Climate Change Initiative (GHG-CCI)

B. Dils et al.

Title Page
Abstract | Introduction
Conclusions | References
Tables | Figures
◀| |▶
◀ ▶
Back | Close
Full Screen / Esc
Printer-friendly Version
Interactive Discussion